A subset of group 3 ILCs in lymph nodes expresses Aire and presents endogenously expressed self-antigen

Tomoyoshi Yamano[1,*]#, Jan Dobes[2,3]#, Matous Voboril[2], Madlen Steinert[1], Tomas Brabec[2], Natalia Ziętara[1], Martina Dobesova[2], Caspar Ohnmacht[4], Martti Laan[5], Part Peterson[5], Vladimir Benes[6], Radislav Sedlacek[7], Rikinari Hanayama[8], Michal Kolar[9], Ludger Klein[1]#* and Dominik Filipp[2]#*

[1] Institute for Immunology, Ludwig-Maximilians-University, Munich, Germany

[2] Laboratory of Immunobiology, Institute of Molecular Genetics of the ASCR, Prague, Czech Republic

[3] Department of Cell Biology, Faculty of Science, Charles University in Prague, Prague, Czech Republic

[4] Helmholtz Zentrum München, Institut für Allergieforschung, Neuherberg, Germany

[5] Institute of Biomedicine and Translational Medicine, University of Tartu, Tartu, Estonia

[6] Genomics Core Facility, EMBL, Services & Technology Unit, Heidelberg, Germany

[7] Czech Centre for Phenogenomics & Laboratory of Transgenic Models of Diseases, Institute of Molecular Genetics of the ASCR, Prague, Czech Republic

[8] Department of Immunology, Kanazawa University Graduate School of Medical Sciences, and WPI Nano Life Science Institute, Kanazawa University, Ishikawa, Japan

[9] Laboratory of Genomics and Bioinformatics, Institute of Molecular Genetics of the ASCR, Prague, Czech Republic

[*] Present address: Department of Immunology, Kanazawa University Graduate School of Medical Sciences, and WPI Nano Life Science Institute, Kanazawa University, Ishikawa, Japan

# These authors contributed equally

*Correspondence to L.K. (ludger.klein@med.lmu.de) or D.F. (dominik.filipp@img.cas.cz)

Running title: Aire-expressing ILC3

SUMMARY

The identity of peripheral Aire-expressing cells remains poorly understood. This study shows that Aire-expressing cells in lymph nodes belong to a novel ILC3 subset with potent APC features. They depend upon Rank, express a distinct Aire-dependent transcriptional signature and efficiently present endogenous self-antigens.

ABSTRACT

The autoimmune regulator (Aire) serves an essential function for T cell tolerance by promoting the 'promiscuous' expression of tissue-restricted antigens (TRAs) in medullary thymic epithelial cells (mTECs). Aire is also detected in rare cells in peripheral lymphoid organs, but the identity of these Aire-expressing cells is poorly understood. Here, we report that the vast majority of Aire protein expressing cells in lymph nodes exhibit typical innate lymphoid cell (ILC) characteristics. These cells express and depend upon RORγt, indicating that they represent a novel subset of group 3 ILCs. Aire expression in ILC3s is independent of cross-talk with adaptive immune cells and requires Rank signaling. Aire$^+$ cells are more frequent among ILC3s of various peripheral lymph nodes as compared to the mucosa draining mesenteric lymph nodes, display a unique Aire-dependent transcriptional signature, express high surface levels of MHCII and co-stimulatory molecules and efficiently present an endogenously expressed antigen to CD4$^+$ T-cells. These findings define a novel subset of group 3 ILCs with potent APC features, suggesting that these cells serve a function in the control of T cell responses.

INTRODUCTION

The crucial function of the Autoimmune Regulator (Aire) in central T cell tolerance through the promotion of 'promiscuous gene expression' in medullary thymic epithelial cells (TECs) is well established (Kyewski and Klein, 2006; Mathis and Benoist, 2007; Peterson et al., 2008). mTECs combine the unique ability to produce thousands of otherwise strictly tissue restricted antigens (TRAs) with the capacity to efficiently present these on MHC class I and II molecules (Anderson et al., 2002; Derbinski et al., 2001; Hinterberger et al., 2010). In humans, AIRE mutations cause the recessively inherited Autoimmune Polyendocrine Syndrome type 1 (APS1) (Husebye et al., 2018) and Aire-deficient mice recapitulate several aspects of APS1 (Anderson et al., 2002; Ramsey et al., 2002).

Aire-deficiency affects the expression of hundreds of TRAs in mTECs (Brennecke et al., 2015; Meredith et al., 2015; Sansom et al., 2014). However, defects in T cell tolerance in $Aire^{-/-}$ mice were also observed for autoantigens whose expression in mTECs was Aire-independent (Anderson et al., 2005; Hubert et al., 2011; Kuroda et al., 2005), suggesting that Aire may coordinate mTEC functions beyond 'promiscuous gene expression'. For example, Aire may regulate mTEC differentiation (Nishikawa et al., 2010; Yano et al., 2008), orchestrate the interplay between mTECs and DCs or T cells through control of cytokine and chemokine expression (Fujikado et al., 2016; Laan et al., 2009; Lei et al., 2011; Yano et al., 2008), influence the directional antigen transfer from mTECs to DCs (Hubert et al., 2011) or directly enhance the antigen-presentation capability of mTECs (Anderson et al., 2005).

Only one of the three hallmarks of AIRE-deficiency in humans, autoimmune polyendocrinopathy, is readily explained by Aire's role(s) in mTECs, whereas the two other key disease manifestations in APS1 patients, candidiasis and ectodermal dystrophy, are more difficult to reconcile with the idea that Aire serves its function(s) exclusively in mTECs. Along these lines, Aire-deficient mice develop several hematopoietic irregularities suggesting that in addition to its thymic function, Aire controls the development of peripheral antigen-presenting cells (APCs) and the activation of marginal zone B-cells (Hassler

et al., 2006). It has been suggested that this reflects a DC-intrinsic role in the regulation of IFN signaling and BAFF production (Lindh et al., 2008).

Further support of Aire being expressed in cells other than mTECs came from fate-mapping studies revealing Aire expression in early embryonic development (Nishikawa et al., 2010). In adult mice, Aire transcripts can be detected in stromal and hematopoietic cells in secondary lymphoid organs and also in non-immune cell types such as spermatogonia (Adamson et al., 2004; Fletcher et al., 2010; Halonen et al., 2001; Heino et al., 2000; Hubert et al., 2008; Poliani et al., 2010; Schaller et al., 2008), but there is some controversy as to how well the presence of Aire mRNA correlates with the actual presence of Aire protein (Adamson et al., 2004; Fletcher et al., 2010; Halonen et al., 2001; Heino et al., 2000; Hubert et al., 2008; Poliani et al., 2010; Schaller et al., 2008). Aire reporter mice have been instrumental in the identification of a unique subset of cells that are referred to as extrathymic Aire-expressing cells (eTACs), a population of hematopoietic APCs that morphologically resemble DCs and co-express EpCAM and CD11c (Gardner et al., 2008; Gardner et al., 2013). A distinct population of Aire expressing DCs has recently also been described in human tonsils (Fergusson et al., 2019). In mice, DC-like eTACs are $MHCII^{+}$, yet lack expression of the co-stimulatory molecules CD80 and CD86. It has been suggested that Aire's function in eTACs is to promote TRA expression and eTACs have been implicated in peripheral tolerance induction in CD4 and CD8 T cells through induction of anergy or clonal deletion, respectively (Gardner et al., 2013).

In sum, the identity of peripheral Aire-expressing cells and the physiological relevance of Aire expression outside of the thymus remain incompletely understood (Gardner et al., 2009). Therefore, we set out to clarify the identity of Aire expressing cells in lymph nodes. We identified three phenotypically distinct subsets of hematopoietic cells that expressed endogenous Aire mRNA, including the previously described $EpCAM^{+}CD11c^{+}$ eTACs. However, Aire protein was exclusively found in an $EpCAM^{-}CD11c^{-}$ cell population. These cells belong to a 'novel' subset of group 3 innate lymphoid cells (ILC3) with potent APC features.

RESULTS

Aire expression in CD11c$^-$EpCAM$^-$RORγt$^+$ lymph node cells

Adig mice carry a transgenic bacterial artificial chromosome encoding for a neo-antigen–GFP fusion protein under control of the *Aire* locus (Gardner et al., 2008). Consistent with previous observations, Aire-GFP expression in lymph node cells from *Adig* mice was restricted to cells with high MHCII surface levels (Figure 1A) (Gardner et al., 2013). Surprisingly, co-staining of EpCAM and CD11c on Aire-GFP$^+$MHCII$^+$ cells revealed that these cells not only contained a population with the reported EpCAM$^+$CD11c$^+$ eTAC phenotype but also harbored an EpCAM$^-$CD11c$^+$ and an EpCAM$^-$CD11c$^-$ subset. This segregation of Aire-reporter$^+$ cells into roughly similar proportions of EpCAM$^+$CD11c$^+$, EpCAM$^-$CD11c$^+$ and EpCAM$^-$CD11c$^-$ cells was confirmed in an independent second Aire-reporter strain (*Aire-HCO*) that carries a transgenic *Aire* gene locus encoding a chimeric influenza hemagglutinin (HA) protein and a human (h)CD2 reporter (Aschenbrenner et al., 2007; Hinterberger et al., 2010) (Figure S1A). Although expression of endogenous Aire mRNA was detectable in all three subsets of Aire-reporter$^+$ lymph node cells from *Adig* and Aire-HCO mice, the levels of Aire transcripts were highest in the EpCAM$^-$CD11c$^-$ subset (Figures 1B and S1B). In these cells, *Aire* mRNA was almost as abundant as in mTECs. Intracellular staining (ICS) demonstrated Aire-protein at levels comparable to those in mTECs in 15-20% of the EpCAM$^-$CD11c$^-$ subset of Aire-reporter$^+$ cells but failed to reveal measurable Aire protein in Aire-GFP$^+$ EpCAM$^+$CD11c$^+$ or EpCAM$^-$ CD11c$^+$ cells (Figures 1C and S1C).

Independent of prior gating on Aire-reporter$^+$ cells, Aire protein positive cells were also detectable by intracellular staining of total lymph node cells (Aire$^+$ LN) from *WT* mice but not *Aire*$^{-/-}$ controls (Figure 1D). These cells were present at similar frequencies in all 'peripheral' lymph nodes tested (axillary, brachial, cervical and inguinal), yet 3- to 4-fold less frequent in mesenteric lymph nodes (Figure S1D). All further experiments, unless otherwise specified, were performed with pooled 'peripheral' LN cells. Aire$^+$ LN cells were uniformly EpCAM$^-$CD11c$^-$ and the surface expression of CD45$^+$ pointed towards a hematopoietic origin (Figure 1D). The frequency of Aire-protein$^+$ LN cells was very low in newborns, increased to a maximum of around 300 per

10^6 LN-cells in two-week old mice before slightly declining and subsequently remaining stable in adult mice (Figure 1E). Aire$^+$ LN cells were detectable in *WT* → *Aire*$^{-/-}$ bone marrow (BM) chimeras, but not in reciprocal *Aire*$^{-/-}$ → *WT* chimeras or *Aire*$^{-/-}$ → *Aire*$^{-/-}$ controls, confirming their BM-origin (Figure 1F). Imaging flow cytometry demonstrated that Aire protein was localized in nuclear dots in Aire$^+$ LN cells, very similar to its sub-cellular distribution in mTECs (Figure 1G) (Abramson et al., 2010; Su et al., 2008).

Screening for expression of characteristic hematopoietic lineage markers indicated that Aire$^+$ LN cells did not express CD3 ('T lineage'), B220 ('B lineage'), Gr1 ('granulocytes/neutrophil lineage'), DX5 ('NK lineage'), PDCA-1 ('plasmacytoid DC lineage'), FcεRI ('mast cells/basophil lineage'), M-CFSR and CD11b ('granulocytes/monocyte lineage'), Siglec F ('eosinophil lineage') and Sca-1 ('HSC marker') (Figure 1H). Together, these observations identified a 'novel' population of Aire-protein$^+$ cells in lymph nodes. Their EpCAM$^-$ CD11c$^-$ phenotype was clearly distinct from the previously described EpCAM$^+$CD11c$^+$ eTACs.

Aire$^+$ lymph node cells display ILC3 characteristics

Consistent with the phenotypic analysis of Aire$^+$ LN cells by surface staining (Figure 1H), transcriptional profiling of lineage specific 'signature genes' showed that these cells expressed negligible levels of transcripts specific for T or B cells as well as cDCs, pDCs, macrophages, granulocytes or neutrophils (Figure 2A). However, we noted that Aire$^+$EpCAM$^-$CD11c$^-$ cells contained relatively high mRNA levels of genes characteristic for innate lymphoid cells (ILCs) and/or ILC precursors such as *Id2*, *Kit*, *Il7r*, *Itga4* and *Itgb7* (Figure 2B) (Robinette et al., 2015; Seehus et al., 2015). ILCs are commonly categorized into three groups based on the transcription factors (TFs) that regulate their development and function (Spits et al., 2013). At the mRNA level, Aire$^+$EpCAM$^-$CD11c$^-$ lymph node cells expressed the ILC3-signature TF RORγt (encoded by *Rorc*), whereas they did not express the ILC1-specific TFs T-bet (encoded by *Tbx21*) or Eomesodermin and only weakly (or not at all) expressed the ILC2-specific transcription factors GATA3 and RORα, respectively (Figure 2B). Of note, Aire$^+$EpCAM$^-$CD11c$^-$ lymph node cells did not express any of the signature cytokines or effector molecules associated

with distinct ILC groups (IFNγ, perforin and granzyme for ILC1/NK cells, IL4, IL5 and IL13 for ILC2s or IL17A and IL22 for ILC3s) (Figure 2B). RORγt protein was readily detectable in Aire-ICS^{+}MHCII^{+} cells from various lymph nodes, whereas GATA3 protein was absent (Figures 2C and S1E).

We next assessed whether Aire^{+}EpCAM^{-}CD11c^{-} LN cells displayed other ILC hallmarks such as lymphoid morphology and Rag-independence. Aire-GFP^{+}MHCII^{+}EpCAM^{-}CD11c^{-} lymph node cells were slightly larger than lymph node Lin^{-}MHCII^{-}Rorc-reporter^{+} ILC3s, yet otherwise shared their typical lymphoid morphology with a regular round shape and a small cytoplasmatic rim (Figure 2D). By contrast, and as previously described, Aire-GFP^{+}EpCAM^{+}CD11c^{+} 'eTACs' displayed cDC-like features such as an irregularly shaped nucleus and a large and vacuolated cytoplasm (Figure 2D) (Gardner et al., 2013). In 1:1 mixed [*Rag2*$^{-/-}$: *WT*] → *WT* BM-chimeras, there was a balanced contribution of *Rag2*$^{-/-}$ and *WT* precursors to the Aire-protein^{+} LN cell population, whereas expectedly, T cells were exclusively derived from *WT* precursors (Figure 2E and S2A). Thus, transcriptional profiling, morphology and Rag-independence supported the idea that Aire^{+} LN cells are ILC3s. Consistent with this, 'classical' flow cytometric gating on ILC3s as lineage-negative RORγt^{+} lymph node cells revealed that around 15 % of these cells express Aire protein (Figure 2F and S2B).

Commonly, group 3 ILCs are classified on the basis of their anatomical distribution, ontogeny, and surface marker expression (Montaldo et al., 2015; Spits et al., 2013). During embryogenesis, lymphoid tissue-inducer (LTi) cells orchestrate the formation of secondary lymphoid organs. These cells are CCR6^{+} and do not express the natural cytotoxicity triggering receptor (NCR) NKp46. Postnatally emerging RORγt^{+} ILC3s can be sub-divided into CCR6^{+}NKp46^{-} 'LTi-like' cells and CCR6^{-} cells. The former are the predominant population in lymph nodes, whereas CCR6^{-} ILC3s are most abundant in mucosal tissues and associated lymphoid structures and are likely to represent a separate lineage that can be further subdivided into NKp46^{-} and NKp46^{+} subsets (Klose et al., 2013). In order to assess whether and how Aire^{+} LN cells fit into these categories, we compared their phenotype with Aire^{-} lymph node ILC3s. Whereas the level of RORγt expression in Aire^{+} cells was similar to 'canonical' LN-ILC3s, they expressed slightly lower CD45

(Figure S2C). Aire^{+} LN cells were also strikingly similar to 'canonical' LN-ILC3s with regards to expression of the transcription factor Id2, surface expression of c-kit and CCR6 as well as lack of NKp46 expression (Figure 2G). However, despite sharing the RORγt^{+}CCR6^{+}NKp46^{-} phenotype with the majority of 'canonical' LN-ILC3s, Aire^{+} LN cells expressed no detectable IL7Rα protein (Figure 2G). Moreover, Aire^{+} LN cells were negative for CD90 and CD4, whereas expression of these molecules was heterogeneous on 'canonical' Aire^{-} ILC3s (Figure 2G). While 'canonical' LN-ILC3s are very abundant in neonates and decrease with age (Jones et al., 2018), Aire^{+} LN cells were very rare at birth, peaked at the time of weaning and slightly declined thereafter (Figure 2H, see also Figure 1E).

Group 3 ILCs strictly depend on RORγt for their differentiation (Eberl et al., 2004; Luci et al., 2009; Satoh-Takayama et al., 2009). To ask whether this likewise applies to peripheral Aire^{+}EpCAM^{-}CD11c^{-} LN cells, we generated 1:1 mixed [*Rorc*$^{-/-}$: *Rorc*$^{+/+}$] → *WT* BM-chimeras. *Rorc*$^{+/+}$ control BM-cells efficiently gave rise to Aire^{+} cells in lymph nodes or spleen. By contrast, *Rorc*$^{-/-}$ precursors failed to do so, while efficiently contributing to the cDC compartment, a control RORγt-independent lineage (Figure 2I).

In sum, these data demonstrated that Aire^{+} LN cells display the key characteristics of group 3 ILCs. While they resemble CCR6^{+}NKp46^{-} lymph node ILC3s in some aspects, lack of surface IL7Rα distinguishes them from 'canonical' ILC3s LN ILC3s. From here on, we will refer to these cells as Aire^{+} ILC3s.

Molecular and cellular requirements for Aire expression in ILC3s

Besides its role as an inducer of 'promiscuous gene expression', Aire has been suggested to control the developmental maturation and survival of mTECs (Gray et al., 2007; Hikosaka et al., 2008; Wang et al., 2012). In order to address whether an incapacity to produce Aire protein in hematopoietic cells that otherwise express Aire would result in perturbations of their differentiation and/or homeostasis, we generated 1:1 mixed [*Aire*$^{-/-}$ Aire-reporter : *Aire*$^{+/+}$ Aire-reporter] → *WT* BM-chimeras. Aire-reporter^{+} cells that had emerged from either *Aire*$^{-/-}$ or *Aire*$^{+/+}$ precursors were present at equal

frequencies. Hence, Aire is unlikely to act as a cell intrinsic developmental or homeostatic regulator of peripheral Aire-expressing cells (Figure 3A).

In thymic epithelial cells, the expression of Aire is orchestrated by NF-κB signals that emanate from activation of receptors of the tumor necrosis factor (TNF) receptor superfamily (Akiyama et al., 2012). These signals converge on a conserved noncoding sequence (CNS1) upstream of the *Aire* coding region that was shown to act as an essential enhancer-element for Aire expression in mTECs (Haljasorg et al., 2015; LaFlam et al., 2015). Aire-ICS^{+} cells were absent from the lymph nodes of *Aire-CNS1*$^{-/-}$ mice (Haljasorg et al., 2015), indicating that the 'gene-proximal' requirements for Aire expression in Aire^{+} ILC3s are very similar to those in mTECs (Figure 3B).

The 'maturation' of mTECs and their concomitant acquisition of an Aire^{+} phenotype as well as the intrathymic licensing of B cells for Aire expression are likewise instigated by cellular cross-talk within the thymic microenvironment, yet differ in the TNF superfamily signaling-axes that are triggered through these interactions. Aire-expression in mTECs is orchestrated by an receptor activator of NF-κB (Rank) signals (Akiyama et al., 2008; Hikosaka et al., 2008). These can emerge from CD4 single-positive (SP) cells and, in the pre- and perinatal phase, from LTi cells and invariant γδ T cells (Roberts et al., 2012; Rossi et al., 2007). By contrast, Aire-expression in thymic B cells crucially involves CD40 signals that exclusively emanate from 'cognate', i.e. MHCII-dependent, interactions with CD4 SP cells (Yamano et al., 2015). In 1:1 mixed [*MHCII*$^{-/-}$: *MHCII*$^{+/+}$] → *WT* BM-chimeras, precursor cells lacking MHCII efficiently gave rise to Aire^{+} ILC3s, indicating that 'cognate' interactions with CD4^{+} T cells were not required for their differentiation (Figure 3C). Consistent with extrinsic signals from T cells or other cells bearing somatically rearranged antigen receptors being dispensable for the differentiation of Aire^{+} ILC3s, Aire-protein^{+} lymph node cells were similarly abundant in *Rag2*$^{-/-}$ mice and *WT* controls and expressed equal amounts of RORγt (Figure S3A, B).

We next addressed which members of the TNF-receptor family were required for Aire-expression in ILC3s. Aire^{+} cells emerged with equal efficacy from either *CD40*$^{-/-}$ or *CD40*$^{+/+}$ precursors in 1:1 mixed [*CD40*$^{-/-}$: *CD40*$^{+/+}$] → *WT* BM-chimeras (Figure 3D). By contrast, Rank-deficiency (*Tnfrs11a*$^{-/-}$) in

hematopoietic precursors resulted in a severe cell-intrinsic defect in their capacity to contribute to the pool of peripheral Aire-protein^{+} ILC3s in 1:1 mixed [*Tnfrs11a*$^{-/-}$: *Tnfrs11a*$^{+/+}$] → *WT* fetal liver-chimeras (Figure 3E). Intriguingly, in this setting, concomitant to being virtually absent from Aire-protein^{+} ILC3s, Rank-deficient cells were strongly over-represented among 'canonical' RORγt^{+}IL7Ra^{+} ILC3s (Figure 3E). A possible explanation for this was that 'canonical' RORγt^{+}IL7Ra^{+} ILC3s under steady-state conditions bear the potential to differentiate into Aire-expressing^{+} ILC3s upon stimulation with Rank-ligand, yet accumulate when their capacity to signal via Rank is genetically ablated. Consistent with such a precursor-progeny relationship between Aire^{-} and Aire^{+} ILC3s, *in vitro* culture of Lin^{-}IL7Ra^{+}MHCII^{+} LN-cells with Rank-ligand expressing stromal cells resulted in the emergence of Aire-expressing cells (Figure 3F). By contrast, an agonistic anti-CD40 antibody failed to do produce a similar effect. Together, these findings indicated that Aire-expression in ILC3s shares several molecular requirements with Aire-expression in mTECs such as the crucial role of the CNS1 enhancer-element and Rank-signaling. However, in contrast to what has been established for mTECs, cellular cross-talk with CD4 T cells or γδ T cells is not necessary for Aire expression by Aire^{+} ILC3s.

Aire orchestrates a distinct genetic program in Aire^{+} ILC3s

RNA-sequencing of Aire^{+} ILC3 cells from wild-type and Aire-deficient mice revealed 707 differentially expressed transcripts (Figure 4A). Out of these, 334 genes were Aire-induced and 373 genes were repressed (Tables S1 and S2). Among Aire-induced transcripts, only 60 genes (approx. 18%) were classified as TRAs according to previously established criteria (Sansom et al., 2014) (Figure 4A). Thus, in contrast to the Aire-induced transcriptome of mTECs, which is highly enriched for TRAs (> 40%) (Anderson et al., 2002; Kyewski and Klein, 2006), Aire-dependent genes in Aire^{+} ILC3s contain a similar fraction of TRAs as any random gene set (about 20%). Independent qPCR analysis of selected Aire-induced (*Col9a3*, retinal TRA; *Clec2g*, corneal TRA; *Vwce,* liver TRA; *Heatr6,* immune system restricted) or Aire-repressed genes (*Prokr2*, neural TRA; Ska3, embryo-restricted) confirmed their Aire-regulated expression in Aire^{+} ILC3s (Figure 4B). Interestingly, Aire-regulated

genes in Aire$^+$ ILC3s and mTECs (Sansom et al., 2014) were largely non-overlapping, that is, only 90 of 707 Aire-regulated transcripts in Aire$^+$ ILC3s were also affected by Aire-deficiency in mTECs. Moreover, a substantial fraction of the 90 genes that were Aire-regulated in both Aire$^+$ ILC3s and mTECs displayed opposing effects when the *Aire* gene was disrupted (Figure 4C). Specifically, of a total of 1732 genes that were up-regulated by Aire in mTECs, only 36 were 'Aire-induced' in Aire$^+$ ILC3s, whereas 29 were down regulated. Of a total of 423 genes that were 'repressed' by Aire in mTECs, only 9 were likewise down-regulated by Aire in Aire$^+$ ILC3s, whereas 16 were upregulated (Figure 4C). Thus, Aire controls a cell-context-dependent distinct transcriptional program in ILC3s.

Direct presentation of endogenous antigen by Aire$^+$ ILC3s

Aire$^+$ LN cells express high surface levels of MHCII (see Figure 1A), and transcriptional profiling indicated that Aire$^+$ ILC3s expressed mRNAs encoding for co-stimulatory or co-inhibitory molecules such as CD80, CD86, CD40, ICOS-ligand and PD-L1 (CD274) (Figure 5A). This indicated that they may harbor substantial APC potential. To relate these findings to 'canonical' ILC3s, we directly compared the surface expression of 'APC-associated' molecules on Aire$^+$ versus Aire$^-$ lymph node ILC3s. Based upon the finding that these two subsets of ILC3s differ in IL7Rα expression, we did so by gating on Aire$^+$IL7Rα^- or Aire$^-$IL7Rα^+ cells among Lin$^-$CD45$^+$RORγt$^+$ LN cells, respectively (Figure 5B). Of note, and in line with our initial observation that Aire$^+$ cells are more abundant in 'peripheral' (p)LNs than in mesenteric LNs (see Figure S1D), Aire$^+$IL7Rα^- cells uniformly represented around 20% of ILC3s in various pLNs, yet were very scarce in mesenteric LNs (Figure S4A). Aire$^+$IL7Rα^- ILC3s displayed homogeneously high surface levels of MHCII, CD80, CD86, CD40, Icos-L and detectable amounts of PD-L1 (Figure 5C). By contrast, with the exception of CD86, surface expression of these molecules was substantially lower or absent on Aire$^-$IL7Ra$^+$ pLN ILC3s (Figure 5C). We confirmed and extended these data by distinguishing Aire$^+$ and Aire$^-$ILC3s through an alternative gating strategy that incorporated their differential expression of MHCII. Specifically, Lin$^-$CD45$^+$RORγt$^+$ cells from LNs

segregated into MHCII$^{lo/int}$IL7Rα^{+} and MHCII^{hi}IL7Rα^{-} cells. Consistent with our previous observations, the latter were far more abundant (30-40%) in pLNs as compared to mesenteric LNs (around 10%) (Figures S4B and S4C), and expression of Aire was exclusively confined to MHCII^{hi}IL7Rα^{-} cells (Figure S4B). MHCII^{hi}IL7Rα^{-} ILC3s spread over a similar bandwidth of RORγt expression as MHCII$^{lo/int}$IL7Rα^{+} ILC3s, yet were slightly lower for CD45 (Figure S4D). Analysis of CD80, CD86, CD40, ICOS-ligand and PD-L1 expression on MHCII^{hi}IL7Rα^{-} and MHCII$^{lo/int}$IL7Rα^{+} cells recapitulated our earlier observations (Figure S4E; compare Figure 5C). Moreover, MHCII^{hi}IL7Rα^{-} Aire^{+} ILC3s were negative for CD4, CD90 and CD25, whereas MHCII$^{lo/int}$IL7Rα^{+} ILC3s were heterogenous in surface CD4 and CD90 (Figure S4F; compare also Figure 2G) and homogeneously positive for CD25 (Figure S4F).

We next asked whether a model self-antigen expressed under the control of the Aire-promoter was 'visible' to specific CD4^{+} T cells in the periphery. To determine if this was the case, we adoptively transferred naïve influenza hemagglutinin (HA)-specific CD4^{+} T cells which were purified from TCR-HA *Rag2*$^{-/-}$ donors together with an equal number of polyclonal 'reference' CD4^{+} T cells into *Aire-HCO* mice, which express HA from a BAC-transgene harboring a modified *Aire* gene locus (Aschenbrenner et al., 2007; Hinterberger et al., 2010). Fourteen days after transfer, HA-specific CD4^{+} T cells were strongly diminished in *Aire-HCO* recipients but not in *WT* controls (Figure 5D), suggesting that the peripheral antigen encounter resulted in the deletion of these cells. Similar results were obtained when *Aire-HCO* → *WT* BM-chimeras or *WT* → *WT* controls were used as recipients, which confirmed that the deletion of TCR-HA cells occurred as a consequence of peripheral HA-expression in the hematopoietic compartment (Figure 5E).

Finally, we directly assessed how efficiently Aire^{+} ILC3s presented an endogenously expressed neo self-antigen on MHCII as compared to mTECs and EpCAM^{+}CD11c^{+} 'eTACs'. To this end, these three cell types were *ex vivo* isolated from *Aire-HCO* mice and cultured together with HA-specific CD4^{+} T cell hybridoma cells which carry an NFAT-GFP reporter gene (Aschenbrenner et al., 2007). As expected, mTECs elicited the strongest response, consistent with their well established capacity to present endogenously expressed

antigens on MHCII (Aschenbrenner et al., 2007; Hinterberger et al., 2010). Strikingly, whereas Aire$^+$ ILC3s also efficiently presented endogenously derived HA, no presentation of HA was detectable with eTACs (Figure 5F) despite similar protein expression of the Aire-reporter (see Figure S1A). Importantly, when mTECs, Aire$^+$ ILC3s, or eTACs were loaded with exogenous HA-peptide, all three cell-types elicited similar responses, excluding the fact that differential expression of MHCII accounted for the observed differences with endogenously expressed antigen (Figure 5F). Together, these observations indicate that Aire$^+$ ILC3s harbor potent APC features and suggest that these cells bear the capacity to present endogenously expressed self-antigens for deletional CD4 T cell tolerance in steady state.

DISCUSSION

Here, we have shown that the vast majority of Aire protein-expressing cells in mouse lymph nodes belong to a 'novel' subset of type 3 innate lymphoid cells. In two independently generated strains of Aire-reporter mice, we initially confirmed that Aire-reporter positive lymph node cells were homogenously MHCII positive and contained cells with the previously reported CD11c$^+$EpCAM$^+$ 'eTAC' phenotype (Gardner et al., 2008). These 'eTACs' as well as a population of Aire-reporter positive CD11c$^+$EpCAM$^-$ cells expressed endogenous Aire mRNA. However, the detectable expression of Aire protein was exclusively restricted to Aire-reporter$^+$CD11c$^-$EpCAM$^-$ cells.

Aire protein expressing lymph node cells displayed the key hallmarks of ILCs, that is, hematopoietic origin and lymphoid morphology, absence of myeloid and/or DC lineage markers, and Rag-independence (Spits et al., 2013). Most importantly, they were found to be RORγt$^+$ and exhibit a strict cell-intrinsic developmental requirement for RORγt, indicating that they represent a 'novel' subset of group 3 ILCs. We propose to refer to these cells as Aire$^+$ ILC3s.

RORγt$^+$ ILCs are commonly classified into two distinct subsets: CCR6$^+$NKp46$^-$ LTi-like cells, which predominantly reside in secondary lymphoid organs and CCR6$^-$NKp46$^-$ ILC3s, which seed mucosal surfaces and represent the immediate precursors of CCR6$^-$NKp46$^+$ ILC3s (Bando et al., 2018; Montaldo et al., 2015). How do Aire$^+$ ILC3s fit into this classification?

Aire$^+$ ILC3s preferentially reside in peripheral lymph nodes, are substantially less frequent in mesenteric lymph nodes, and are not found in the intestine. By their CCR6$^+$NKp46$^-$ phenotype, they resemble LTi-like cells. However, in distinction to the majority of Lin$^-$RORγt$^+$ lymph node ILC3s, they express the IL7 receptor at levels that are substantially lower or undetectable. The expression of the IL7Rα is frequently used as a criterion to define ILCs in gating strategies, which, besides the absence of Aire$^+$ ILC3s from the intestine and their low frequency in mesenteric lymph nodes, may explain why Aire expression has not been noticed in transcriptomic analyses of ILC subsets (Gury-BenAri et al., 2016; Robinette et al., 2015).

In mixed fetal liver chimeras, RANK-deficient cells failed to give rise to Aire$^+$ ILC3s, yet were greatly overrepresented among 'canonical' RORγt$^+$IL7Rα$^+$ ILC3s. Together with the finding that stimulation of the RANK pathway induces Aire expression in RORγt$^+$IL7Rα$^+$ lymph node ILC3s *in vitro*, this is consistent with a precursor progeny relationship between Aire$^-$ MHCII$^{lo/+}$IL7Rα$^+$ and Aire$^+$MHCII^{hi}IL7Rα$^-$ ILC3s. Interestingly, it was recently reported that the RANK signaling axis negatively regulates the abundance and effector functions of intestinal CCR6$^+$ ILC3s (Bando et al., 2018). In conjunction with our findings, this suggests that both in the lymph node as well as in the intestine, ILC3s receive 'tonic' RANK stimulation and begs the question of why Aire$^+$ ILC3s are solely found in lymph nodes. It cannot be excluded that RANK stimulated intestinal ILC3s up-regulate Aire, yet egress from mucosal sites to mucosa draining lymph nodes (Mackley et al., 2015). However, given that the frequency of Aire$^+$ ILC3s is lower in mesenteric as compared to peripheral lymph nodes, it appears more likely that these cells differentiate from Aire$^-$ precursors *in situ*.

The precise cellular context of the RANK signals that underlie Aire induction in ILC3s remains to be established. The RANK dependence of Aire expression in ILC3s resembles the crucial requirement for RANK signaling during induction of Aire in mTECs. For mTEC 'maturation', RANK signals can be supplied by CD4 SP cells and, in a partially redundant manner, by invariant γδ T cells, iNKT cells and LTi cells (Akiyama et al., 2012; Roberts et al., 2012). Aire$^+$ ILC3s are present in 'normal' numbers in Rag$^{-/-}$ mice indicating that in contrast to the modalities of Aire induction in mTECs or thymic B cells

(Yamano et al., 2015), cross-talk with cells that bear somatically rearranged antigen receptors is dispensable for their differentiation. Instead, ILC3s themselves may provide critical RANK signals through homotypic cellular interactions (Bando et al., 2018).

Besides the high surface levels of MHCII, and in distinction to Aire$^-$ MHCII$^{lo/+}$IL7Rα$^+$ lymph node ILC3s, Aire$^+$ ILC3s express a variety of T cell co-stimulatory molecules, which is consistent with accruing evidence that ILC3s can serve as APCs. We still lack a coherent model whether and how such cognate interactions of CD4$^+$ T cells with antigen presenting ILC3s result in tolerance versus immunity. On the one hand, the selective ablation of MHCII molecules on ILC3s lead to impaired tolerance to commensal microbiota and development of inflammatory bowel disease (Hepworth et al., 2015; Hepworth et al., 2013). On the other hand, other reports showed that MHCII deficiency on ILC3s failed to promote spontaneous immune dysregulation in the intestine, yet resulted in impaired T and B cell responses to 'foreign' antigen (von Burg et al., 2014). In the latter situation, the immunogenic APC function of ILC3s was ascribed to their up-regulation of co-stimulatory molecules by inflammatory cytokines such as IL1. Importantly, these studies concurred on the absence of co-stimulatory molecules on ILC3s in the steady state, and indeed we found that this applies to the major population of MHCII$^{lo/+}$IL7Rα$^+$ ILC3s. Aire$^+$ ILC3s, however, which represent approximately one fifth of Lin$^-$ RORγt$^+$ cells, 'constitutively' express an array of co-stimulatory and co-inhibitory molecules such as CD80, CD40 and PD-L1. We believe that this went unnoticed in previous studies owing to the inclusion of IL7Rα and/or CD4 in the phenotypic definition of ILC3s (Hepworth et al., 2015; Hepworth et al., 2013; Stoppelenburg et al., 2014).

Aire$^+$ ILC3s, in contrast to Aire-reporter$^+$CD11c$^+$EpCAM$^+$ eTACs, efficiently presented an endogenously expressed antigen on MHCII. This reveals another striking similarity in the cell biology of ILC3s and mTECs, adding to the expression of Aire as such, its dependence on RANK signaling and the previously described control of MHCII in ILC3s through CIITA promoter elements which are otherwise used only in TECs (Hepworth et al., 2015). In mTECs, endogenous MHCII loading supports central tolerance by facilitating the tolerogenic presentation of endogenously expressed TRAs (Hinterberger

et al., 2010; Klein et al., 2014; Nedjic et al., 2009), and it will be interesting to see whether similar pathways of 'unconventional' MHCII loading are also used by Aire$^+$ ILC3s. HA-specific CD4 T cells were subject to clonal deletion upon adoptive transfer into *Aire-HCO* → *WT* BM-chimeras, indicating that expression of HA in cells of the hematopoietic compartment induced peripheral tolerance. The differential efficacy of HA presentation by either Aire$^+$ ILC3s or eTACs *in vitro* supports a scenario whereby this deletional mode of tolerance may result from the direct presentation of HA by Aire$^+$ ILC3s. However, alternative explanations such as antigen handover from Aire$^+$ ILC3s to other APCs or the expression of HA in another hematopoietic cell type cannot currently be excluded.

It remains to be seen whether the onset of Aire expression is of true physiological significance or merely marks a stage of ILC3 differentiation where these cells acquire potent APC features. Several hundred genes are affected by the absence of Aire in Aire$^+$ ILC3s, but in contrast to 'promiscuously' expressed genes in mTECs, these are not enriched in TRAs. It is possible that Aire influences crucial features of ILC3s that are unrelated to the promotion of TRA expression. For instance, Aire has been suggested to control chemokine production (Laan et al., 2009; Lei et al., 2011), differentiation (Hikosaka et al., 2008) and antigen presentation machinery of mTECs (Anderson et al., 2005). It will be interesting to address these possibilities in the context of Aire$^+$ ILC3s.

In summary, our work identifies a 'novel' ILC3 subset that expresses Aire and displays potent APC features. We found striking similarities in the molecular and cellular requirements underlying Aire expression in ILC3s and mTECs. However, whereas Aire in mTECs is dependent on cross-talk with cells of the adaptive immune system, its expression in ILC3s occurs independently of T or B cells, revealing a novel autonomously programmed feature of ILCs. Further work is needed to dissect the role of Aire$^+$ ILC3s in the control of peripheral T cell responses.

AUTHOR CONTRIBUTIONS

T.Y. and J.D. carried out the majority of experiments. M.V., M.S., T.B., N.Z. and M.D. contributed to individual experiments. C.O., M.L., P.P., R.S. provided mice and important research material. V.B. conducted the RNA-seq library preparation and sequencing. M.K. conducted the RNA-seq analysis. L.K. and D.F. designed experiments and wrote the manuscript.

ACKNOWLEDGEMENTS

This work was supported by the Deutsche Forschungsgemeinschaft (KL 1228/6-1 to L.K. and SFB 1054, project part A01 to L.K. and N.Z. and IRTG to L.K. and M.S.) and grant 16-26143S from The Grant Agency of Czech Republic (to D.F.). T.Y was supported by the Leading Initiative for Excellent Young Researchers from the Japan Society for the Promotion of Science. J.D. was supported by grant No. 900214 of The Grant Agency of Charles University and an EFIS short-term fellowship. R.S. was supported by LM2015040, CZ.1.05/2.1.00/19.0395 and LQ1604 grants funded by the Ministry of Education, Youth and Sports and the European Regional Development Fund. We wish to thank C. Federle for expert technical assistance. We would also like to thank L. Richter from the FlowCyt Core Facility of the Biomedical Center, Munich, Z. Cimburek and M. Sima (Flow Cytometry Unit, Institute of Molecular Genetics, Prague) for assistance with Flow Cytometry and Imaging Flow Cytometry, and M.S. Anderson (University of California San Francisco) who kindly provided *Adig* mice. The authors declare no competing financial interests.

MATERIALS AND METHODS

Mice

Adig (Gardner et al., 2008), Aire-HCO (Hinterberger et al., 2010), Aire$^{-/-}$ (Ramsey et al., 2002), Aire-CNS1$^{-/-}$ (Haljasorg et al., 2015), TCR-HA (Kirberg et al., 1994), Cd40$^{-/-}$ (Kawabe et al., 1994), Rag2$^{-/-}$ (Hao and Rajewsky, 2001), Rorc$^{-/-}$ (Eberl et al., 2004) Rorc-EGFP (Lochner et al., 2008) and Tnfrs11a$^{-/-}$ (Li et al., 2000) mice have been described previously. Aire$^{-/-}$ and Adig mice were backcrossed onto BALB/c background for ≥ 10 generations. Animal studies were approved by local authorities (Regierung von Oberbayern Az. 02-17-193 and the Ethical committee of the Czech Academy of Sciences).

Preparation of lymph node single cell suspension

Unless stated otherwise, experiments were performed with pooled peripheral LNs (axillary, brachial, inguinal, cervical). LNs were pierced with a needle and enzymatically digested with 0.1 mg/ml Dispase (Gibco) in RPMI. After incubation at 37°C for 10 minutes, the supernatant was replenished and cell suspension were homogenized by gently pipetting up and down. To stop the digestion, the supernatant was adjusted to 3% FCS and 2mM EDTA and gently spun down (4°C, 300g, 5 min). The procedure was repeated until all clumping was removed. In the experiment shown in Figure S4, LNs were digested in the presence of 0.5U/ml Liberase (Roche). The cell suspensions were then resuspended in PBS containing 3% FCS and 2mM EDTA and used for further analysis.

Flow cytometry

Single cell suspensions of digested LNs were surface stained according to standard procedures. For intracellular Aire or RORγt staining, cells were fixed and permeabilized using reagents from the Foxp3 staining kit *(eBioscience) and stained with* anti Aire mAb 5H12 (eBioscience) conjugated to Alexa Fluor 660, Alexa Fluor 488 or FITC or PE-conjugated RORγt mAb B2D (eBioscience). Cells were analyzed or sorted using a BD FACSCANTOII or LSRII flow cytometer or BD FACSAriaFusion or BD Influx cell sorters.

Imaging flow cytometry

LN cells were prepared by enzymatic digestion. Thymic stroma cells were prepared by enzymatic digestion and density fractionation. Cells were stained for surface markers, fixed and permeabilized*, stained with* Alexa Fluor 660-conjugated mAb, Alexa Fluor 488-conjugated mAb 5H12 (eBioscience) or PE-conjugated RORγt mAb B2D (eBioscience). DAPI was added immediately prior to analysis. Images were acquired using the ImageStream imaging flow cytometer (Amnis) and data was analyzed with the Ideas 6.0 software.

***In vitro* stimulation of ILC3s**

LN cells from Aire-HCO mice were prepared by enzymatic digestion. B cells and T cells were depleted with biotin-conjugated anti-B220, anti-TCRb, and anti-biotin MicroBeads (Miltenyi Biotech). Lineage negative (CD3, CD11c and CD19), hCD2 negative, $IL7Ra^{+}MHCII^{+}$ positive cells were sorted. Sorted cells (4×10^4) were cultured for 3 days together with 2×10^4 irradiated (3000 rad) *ST2 or ST2-RankL (Nutt et al., 1999)* mouse BM *stroma cells in flat bottom 96-well plates. Where indicated,* agonistic anti-CD40 mAb (FGK45, *Bio X Cell)* (10ug/ml) was added.

RNA-sequencing

Total mRNA was extracted from $Lin^{-}CD45^{+}MHCII^{high}CD80^{+}$ cells using the RNeasy Plus Microkit (Qiagen). The quality of the isolated RNA was controlled by Bioanalyzer 2100 electrophoresis (Agilent). RNA-seq libraries were prepared by the EMBL Genomics core facility in Heidelberg, Germany using a NEXTflex rapid illumina RNA-Seq library prep kit (Bio Scientific) after polyA enrichment with NEXTflex Poly(A) Beads (Bio Scientific), starting with ~1-5 pg of total RNA. Sequencing was performed on an Illumina NextSeq 500 sequencer (Illumina). Low quality reads and adaptor sequences were trimmed out using cutadapt (CITE). Reads mapping to ribosomal RNA were filtered out using SortMeRNA (CITE). Preprocessed mRNA reads were mapped to the mouse genome (BALB/cJ) from Ensembl version 86 (CITE, Mus_musculus_balbcj.BALB_cJ_v1.dna_sm.toplevel.fa) using GSNAP version 2017-02-25 (CITE). Gene annotations were downloaded from

Ensembl (Mus_musculus_balbcj.BALB_cJ_v1.86.gff3). DESeq2 version 1.14.1 (CITE) was used for feature counting, data normalization, and comparison of the different groups. Differentially expressed genes were selected based on Storey's q-value < 0.05 and at least 1.5-fold change in transcription activity. For the construction of heat-maps, FPKM-normalized counts were used. The raw sequencing data was deposited at the ArrayExpress database (http://www.ebi.ac.uk/arrayexpress) under accession number E-MTAB-7088.

Quantitative PCR

Total mRNA was extracted from cells using the RNeasy Plus Microkit (Qiagen). Reverse transcription was performed using random primers (Thermo) and RevertAid reverse transcriptase (Thermo). Primers used in the assay are listed in the key resource table. Gene expression was determined by quantitative PCR reaction using Sybr green and LC480-II cycler (Roche) and quantified using the relative quantification method (Pfaffl, 2001).

Antigen-presentation assay

1×10^4 HA-TCR hybridoma cells (A5 cells) were co-cultured with 2×10^3 APCs in 200 µl Iscove´s modified Dulbecco´s medium (IMDM) supplemented with 1% FCS. After 17 h, cells were harvested and GFP expression of A5 cells was measured by flow cytometry.

Bone marrow and fetal liver chimeras

Bone marrow was depleted of B and T cells using biotinylated mAbs to B220 and TCRβ and streptavidin MACS beads (Miltenyi Biotech). Recipient mice were irradiated with 2×450 rad and reconstituted with 1×10^7 bone marrow cells. For the generation of mixed chimeras, congenically marked BM or fetal liver cells from Rag2$^{-/-}$ (CD45.1$^{+/+}$), MHCII$^{-/-}$, RORc$^{-/-}$, CD40$^{-/-}$ or Tnfrsf11a$^{-/-}$ mice (CD45.2$^{+/+}$), and BM or fetal liver cells from WT mice of matching congenic genotype were mixed at a ratio of 1:1 (5×10^6 each) and intravenously injected into lethally irradiated recipient mice (CD45.1$^{+/-}$ CD45.2$^{+/-}$).

Adoptive T cell transfer

Single cell suspensions of LN cells from HA-TCR-RAG2$^{-/-}$ (CD45.1) and WT mice (CD45.2) were prepared. LN T cells from WT mice were enriched with biotin-conjugated anti-CD4 and anti-SAV MicroBeads (Miltenyi Biotech) according to standard procedures. LN T cells were mixed (5×10^6) at a ratio of 1:1 and i.v. injected into recipient mice (CD45.1$^{+/-}$ CD45.2$^{+/-}$). After 14 days, the LNs were collected and single cell suspensions were analyzed by flow cytometry.

Supplemental Material

Supplementary Figure 1 Phenotype of Aire expressing cells in lymph nodes.

Supplementary Figure 2 Representative gating strategies of Aire$^+$ ILC3 cells.

Supplementary Figure 3 Rag2 is dispensable for Aire$^+$ ILC3 development.

Supplementary Figure 4 MHCII^{high}IL7Rα$^-$ ILC3s express the Aire-reporter and co-stimulatory molecules

Supplementary Table 1 Aire-induced genes in Aire$^+$ ILC3 cells.

Supplementary Table 2 Aire-repressed genes in Aire$^+$ ILC3 cells.

FIGURE LEGENDS

Figure 1. Phenotype of Aire expressing cells in lymph nodes. (A) Expression of GFP and MHCII in pooled lymph node cells from *Adig* Aire-reporter mice and *WT* controls. The dot plot on the right shows staining for CD11c and EpCAM on gated Aire-GFP$^+$MHCII$^+$ cells. The average frequency of cells in the respective gates is indicated (representative of n ≥ 4 each). (B) Aire mRNA in subsets of Aire-GFP$^+$ lymph node cells from *Adig* mice sorted according to expression of CD11c and EpCAM as in (A) compared to mTECs and cTECs. Data shows mean values ± SEM of triplicates (AU; arbitrary units). (C) Intracellular staining (ICS) for Aire protein in subsets of Aire-GFP$^+$ lymph node cells from *Adig* mice. Cells were gated according to the expression of CD11c and EpCAM as in (A). mTECs serving as a positive control were gated as CD45$^-$EpCAM$^+$MHCII$^+$ expressing cells. The average frequency ± SEM of Aire-ICS$^+$ cells is indicated (n = 4). (D) ICS for Aire protein and surface expression of MHCII in total lymph node cells from *WT* and *Aire*$^{-/-}$ mice. Histograms on the right show staining for CD11c, EpCAM and CD45 on gated Aire-ICS$^+$MHCII$^+$ cells (representative of n ≥ 5). (E) Number of Aire$^+$ LN cells per 10^6 total peripheral lymph node cells in mice of the indicated age (n ≥ 3 each, 0 weeks = 4 day old). (F) ICS for Aire protein and surface expression of MHCII in total lymph node cells from *Aire*$^{-/-}$ → *Aire*$^{-/-}$, *Aire*$^{-/-}$ → *WT* or *WT* → *Aire*$^{-/-}$ BM chimeras (representative of n ≥ 4 each). (G) Nuclear localization of Aire protein and surface marker expression in Aire expressing lymph node cells or mTECs visualized by imaging flow cytometry. (H) Expression of hematopoietic lineage-specific surface markers on gated Aire-GFP$^+$MHCII$^+$CD11c$^-$EpCAM$^-$ lymph node cells from *Adig* mice (representative of n ≥ 4).

Figure 2. Peripheral Aire$^+$ cells display ILC3 characteristics. RNA sequencing analysis of hematopoietic lineage-specific signature genes (A) and ILC signature genes (B) in flow cytometrically enriched Aire$^+$ LN cells mice as described in the Methods section. (C) MHCII$^+$Aire-ICS$^+$ LN cells (blue dots) back-gated on total Lin$^-$ (CD3, CD19, B220, Gr-1, CD11c and CD11b) LN cells (grey dots) co-stained (ICS) for RORγt and Gata3 (representative of

n=3). (D) Cytospins of sorted Aire-GFP$^+$MHCII$^+$CD11c$^-$EpCAM$^-$ LN cells, 'canonical' LN ILC3s (Lin$^-$MHCII$^-$RORγt$^+$IL7Rα$^+$) and eTACs (Aire-GFP$^+$MHCII$^+$EpCAM$^+$ CD11c$^+$). (E) Contribution of *WT* and *Rag2*$^{-/-}$ precursor cells to Aire-ICS$^+$ LN cells (gated as in Figure 1D) or CD3$^+$ T cells in 1:1 mixed [*Rag2*$^{-/-}$: *WT*] → *WT* BM-chimeras (n = 6). (F) Gating strategy for Lin$^-$ (Lin1: CD3, CD19, B220, Gr-1; Lin 2: CD11c and CD11b) RORγt$^+$ LN ILC3s and expression of Aire by ICS. See Figure S2B for details. (G) Intracellular staining for Id2 protein and surface expression of c-kit, CCR6, NKp46, IL7Rα, CD90 (Thy1) and CD4 in Aire$^+$ (filled blue histogram) and Aire$^-$ (open orange histogram) ILC3s, gated as in (F) (representative of n=3). (H) Number of 'canonical' LN ILC3s (orange) and Aire$^+$ ILC3s (blue) gated as in (F) from 4 day- and 6-week-old animals (n=4). (I) Contribution of *Rorc*$^{+/+}$ and *Rorc*$^{-/-}$ precursor cells to Aire-ICS$^+$ cells in LN or spleen or to DCs in 1:1 mixed [*Rorc*$^{+/+}$: *Rorc*$^{-/-}$] → *WT* BM-chimeras (n = 7).

Figure 3. Molecular and cellular requirements for Aire expression in Aire$^+$ILC3s. (A) Contribution of *Aire*$^{+/+}$ and *Aire*$^{-/-}$ precursor cells to Aire-reporter$^+$ lymph node cells or DCs in 1:1 mixed [*Aire*$^{+/+}$ *Aire-HCO* : *Aire*$^{-/-}$ *Aire*$^{+/+}$ *Aire-HCO*] → *WT* BM-chimeras (n = 5). (B) Intracellular staining (ICS) for Aire protein and surface expression of MHCII in total lymph node cells from *WT* controls and *Aire-CNS1*$^{-/-}$ mice (representative of n=6 each). (C) Number of Aire-ICS$^+$MHCII$^+$ cells per 10^6 total lymph node cells in *WT* controls and *Aire-CNS1*$^{-/-}$ mice. (D) Contribution of *MHCII*$^{+/+}$ and *MHCII*$^{-/-}$ precursor cells to Aire$^+$ ILC3s or DCs in 1:1 mixed [*MHCII*$^{+/+}$: *MHCII*$^{-/-}$] → *WT* BM-chimeras (n = 6). (E) Contribution of *Cd40*$^{+/+}$ and *Cd40*$^{-/-}$ precursor cells to Aire$^+$ ILC3s or DCs in 1:1 mixed [*Cd40*$^{+/+}$: *Cd40*$^{-/-}$] → *WT* BM-chimeras (n = 6). (F) Contribution of *Tnfrsf11a*$^{+/+}$ and *Tnfrsf11a*$^{-/-}$ precursor cells to Aire$^+$ ILC3s, 'canonical' ILC3s (Lin$^-$RORγt$^+$IL7Rα$^+$) or DCs in 1:1 mixed [*Tnfrsf11a*$^{+/+}$: *Tnfrsf11a*$^{-/-}$] → *WT* fetal liver chimeras (n = 9). (G) Aire-reporter expression in 'canonical' IL7Rα$^+$ LN ILC3s after *in vitro* culture of 3 days with ST2 cells with or w/o agonistic anti–CD40 antibody or ST2-RankL cells (representative of n=3 each).

Figure 4. Aire orchestrates a distinct genetic program in Aire$^+$ ILC3s. (A) RNA-sequencing data from Lin$^-$MHCII^{hi}CD80$^+$ cells from *Aire*$^{+/+}$ and *Aire*$^{-/-}$ mice. Genes encoding for TRAs are colored in red. Fold-change cutoff: 1.5; p-value: 0.05 (indicated by a dashed line). (B) Quantitative PCR analysis of mRNA expression of differentially expressed genes selected from (A). Data show mean values ± SD of three independent experiments. (C) Comparison of Aire-dependent gene expression in Aire$^+$ ILC3s and mTECs. Genes that are upregulated (depicted in red; 1732 genes) or downregulated (depicted in blue; 423 genes) by Aire in mTECs by at least 1.5-fold were projected onto the volcano plot shown in (A).

Figure 5. Aire$^+$ ILC3s display potent APC features and directly present endogenous antigen on MHCII. (A) RNA sequencing expression data of genes involved in MHCII-restricted antigen presentation or encoding for co-stimulatory/-inhibitory molecules in Aire$^+$ ILC3s. (B) Gating strategy and frequency of Aire$^+$IL7Rα^- and Aire$^-$IL7Rα^+ cells among Lin$^-$RORγt-ICS$^+$CD45$^+$ cells in pooled peripheral (p)LNs (Lin1: CD3, CD19, B220, Gr-1; Lin 2: CD11c and CD11b) (C) Comparative FACS analysis of surface expression of MHCII and co-stimulatory molecules on Aire$^+$IL7Rα^- ILC3s (filled blue) and Aire$^-$ IL7Rα^+ 'canonical' ILC3s (open black) pLN cells (representative of n ≥ 3). (D) Peripheral deletion of HA-specific CD4 T cells upon adoptive transfer into *Aire-HCO* but not *WT* control mice (n = 6 each). (E) Peripheral deletion of HA-specific CD4 T cells upon adoptive transfer into [*Aire-HCO* → *WT*] but not [*WT* → *WT*] BM chimeric mice (n = 6 each). (F) GFP expression in HA-specific CD4$^+$ NFAT-GFP-reporter hybridoma cells (A5) after 16h co-culture with mTECs, Aire$^+$ ILC3s (Aire-hCD2$^+$MHCII$^+$CD11c$^-$EpCAM$^-$ LN cells) or eTACS (Aire-hCD2$^+$MHCII$^+$CD11c$^+$EpCAM$^+$ LN cells) from Aire–HCO mice without (upper row) or with (lower row) exogenous HA-peptide. Filled grey histograms are from A5 cells that were cultured alone (Representative of three experiments with pooled cells from n ≥ 3).

REFERENCES

Abramson, J., M. Giraud, C. Benoist, and D. Mathis. 2010. Aire's partners in the molecular control of immunological tolerance. *Cell* 140:123-135.

Adamson, K.A., S.H. Pearce, J.R. Lamb, J.R. Seckl, and S.E. Howie. 2004. A comparative study of mRNA and protein expression of the autoimmune regulator gene (Aire) in embryonic and adult murine tissues. *J Pathol* 202:180-187.

Akiyama, T., Y. Shimo, H. Yanai, J. Qin, D. Ohshima, Y. Maruyama, Y. Asaumi, J. Kitazawa, H. Takayanagi, J.M. Penninger, M. Matsumoto, T. Nitta, Y. Takahama, and J. Inoue. 2008. The tumor necrosis factor family receptors RANK and CD40 cooperatively establish the thymic medullary microenvironment and self-tolerance. *Immunity* 29:423-437.

Akiyama, T., M. Shinzawa, and N. Akiyama. 2012. TNF receptor family signaling in the development and functions of medullary thymic epithelial cells. *Front Immunol* 3:278.

Anderson, M.S., E.S. Venanzi, Z. Chen, S.P. Berzins, C. Benoist, and D. Mathis. 2005. The cellular mechanism of Aire control of T cell tolerance. *Immunity* 23:227-239.

Anderson, M.S., E.S. Venanzi, L. Klein, Z. Chen, S.P. Berzins, S.J. Turley, H. von Boehmer, R. Bronson, A. Dierich, C. Benoist, and D. Mathis. 2002. Projection of an immunological self shadow within the thymus by the aire protein. *Science* 298:1395-1401.

Aschenbrenner, K., L.M. D'Cruz, E.H. Vollmann, M. Hinterberger, J. Emmerich, L.K. Swee, A. Rolink, and L. Klein. 2007. Selection of Foxp3+ regulatory T cells specific for self antigen expressed and presented by Aire+ medullary thymic epithelial cells. *Nat Immunol* 8:351-358.

Bando, J.K., S. Gilfillan, C. Song, K.G. McDonald, S.C. Huang, R.D. Newberry, Y. Kobayashi, D.S.J. Allan, J.R. Carlyle, M. Cella, and M. Colonna. 2018. The Tumor Necrosis Factor Superfamily Member RANKL Suppresses Effector Cytokine Production in Group 3 Innate Lymphoid Cells. *Immunity* 48:1208-1219 e1204.

Brennecke, P., A. Reyes, S. Pinto, K. Rattay, M. Nguyen, R. Küchler, W. Huber, B. Kyewski, and L.M. Steinmetz. 2015. Single-cell transcriptome analysis reveals coordinated ectopic gene-expression patterns in medullary thymic epithelial cells. *Nat Immunol* 16:933-941.

Derbinski, J., A. Schulte, B. Kyewski, and L. Klein. 2001. Promiscuous gene expression in medullary thymic epithelial cells mirrors the peripheral self. *Nat Immunol* 2:1032-1039.

Eberl, G., S. Marmon, M.J. Sunshine, P.D. Rennert, Y. Choi, and D.R. Littman. 2004. An essential function for the nuclear receptor RORgamma(t) in the generation of fetal lymphoid tissue inducer cells. *Nat Immunol* 5:64-73.

Fergusson, J.R., Morgan, M.D., Bruchard, M., Huitema, L., Heesters, B.A., van Unen, V., van Hamburg, J.P., van der Wel, N.N., Picavet, D., Koning, F., Tas, S.W., Anderson, M.S., Marioni, J.C., Holländer, G.A., and Spits, H. 2019. Maturing Human CD127+ CCR7+ PDL1+ Dendritic Cells Express AIRE in the Absence of Tissue Restricted Antigens. *Front Immunol* 9:2902.

Fletcher, A.L., V. Lukacs-Kornek, E.D. Reynoso, S.E. Pinner, A. Bellemare-Pelletier, M.S. Curry, A.R. Collier, R.L. Boyd, and S.J. Turley. 2010. Lymph node fibroblastic reticular cells directly present peripheral tissue antigen under steady-state and inflammatory conditions. *J Exp Med* 207:689-697.

Fujikado, N., A.O. Mann, K. Bansal, K.R. Romito, E.M.N. Ferre, S.D. Rosenzweig, M.S. Lionakis, C. Benoist, and D. Mathis. 2016. Aire Inhibits the Generation

of a Perinatal Population of Interleukin-17A-Producing γδ T Cells to Promote Immunologic Tolerance. *Immunity* 45:999-1012.

Gardner, J.M., J.J. Devoss, R.S. Friedman, D.J. Wong, Y.X. Tan, X. Zhou, K.P. Johannes, M.A. Su, H.Y. Chang, M.F. Krummel, and M.S. Anderson. 2008. Deletional tolerance mediated by extrathymic Aire-expressing cells. *Science* 321:843-847.

Gardner, J.M., A.L. Fletcher, M.S. Anderson, and S.J. Turley. 2009. AIRE in the thymus and beyond. *Curr Opin Immunol* 21:582-589.

Gardner, J.M., T.C. Metzger, E.J. McMahon, B.B. Au-Yeung, A.K. Krawisz, W. Lu, J.D. Price, K.P. Johannes, A.T. Satpathy, K.M. Murphy, K.V. Tarbell, A. Weiss, and M.S. Anderson. 2013. Extrathymic Aire-expressing cells are a distinct bone marrow-derived population that induce functional inactivation of $CD4^+$ T cells. *Immunity* 39:560-572.

Gray, D., J. Abramson, C. Benoist, and D. Mathis. 2007. Proliferative arrest and rapid turnover of thymic epithelial cells expressing Aire. *J Exp Med* 204:2521-2528.

Gury-BenAri, M., C.A. Thaiss, N. Serafini, D.R. Winter, A. Giladi, D. Lara-Astiaso, M. Levy, T.M. Salame, A. Weiner, E. David, H. Shapiro, M. Dori-Bachash, M. Pevsner-Fischer, E. Lorenzo-Vivas, H. Keren-Shaul, F. Paul, A. Harmelin, G. Eberl, S. Itzkovitz, A. Tanay, J.P. Di Santo, E. Elinav, and I. Amit. 2016. The Spectrum and Regulatory Landscape of Intestinal Innate Lymphoid Cells Are Shaped by the Microbiome. *Cell* 166:1231-1246 e1213.

Haljasorg, U., R. Bichele, M. Saare, M. Guha, J. Maslovskaja, K. Kond, A. Remm, M. Pihlap, L. Tomson, K. Kisand, M. Laan, and P. Peterson. 2015. A highly conserved NF-kappaB-responsive enhancer is critical for thymic expression of Aire in mice. *Eur J Immunol* 45:3246-3256.

Halonen, M., M. Pelto-Huikko, P. Eskelin, L. Peltonen, I. Ulmanen, and M. Kolmer. 2001. Subcellular location and expression pattern of autoimmune regulator (Aire), the mouse orthologue for human gene defective in autoimmune polyendocrinopathy candidiasis ectodermal dystrophy (APECED). *J Histochem Cytochem* 49:197-208.

Hao, Z., and K. Rajewsky. 2001. Homeostasis of peripheral B cells in the absence of B cell influx from the bone marrow. *J Exp Med* 194:1151-1164.

Hassler, S., C. Ramsey, M.C. Karlsson, D. Larsson, B. Herrmann, B. Rozell, M. Backheden, L. Peltonen, O. Kampe, and O. Winqvist. 2006. Aire-deficient mice develop hematopoetic irregularities and marginal zone B-cell lymphoma. *Blood* 108:1941-1948.

Heino, M., P. Peterson, N. Sillanpää, S. Guérin, L. Wu, G. Anderson, H.S. Scott, S.E. Antonarakis, J. Kudoh, N. Shimizu, E.J. Jenkinson, P. Naquet, and K.J. Krohn. 2000. RNA and protein expression of the murine autoimmune regulator gene (Aire) in normal, RelB-deficient and in NOD mouse. *Eur J Immunol* 30:1884-1893.

Hepworth, M.R., T.C. Fung, S.H. Masur, J.R. Kelsen, F.M. McConnell, J. Dubrot, D.R. Withers, S. Hugues, M.A. Farrar, W. Reith, G. Eberl, R.N. Baldassano, T.M. Laufer, C.O. Elson, and G.F. Sonnenberg. 2015. Immune tolerance. Group 3 innate lymphoid cells mediate intestinal selection of commensal bacteria-specific CD4(+) T cells. *Science* 348:1031-1035.

Hepworth, M.R., L.A. Monticelli, T.C. Fung, C.G. Ziegler, S. Grunberg, R. Sinha, A.R. Mantegazza, H.L. Ma, A. Crawford, J.M. Angelosanto, E.J. Wherry, P.A. Koni, F.D. Bushman, C.O. Elson, G. Eberl, D. Artis, and G.F. Sonnenberg. 2013. Innate lymphoid cells regulate CD4+ T-cell responses to intestinal commensal bacteria. *Nature* 498:113-117.

Hikosaka, Y., T. Nitta, I. Ohigashi, K. Yano, N. Ishimaru, Y. Hayashi, M. Matsumoto, K. Matsuo, J.M. Penninger, H. Takayanagi, Y. Yokota, H. Yamada, Y. Yoshikai, J. Inoue, T. Akiyama, and Y. Takahama. 2008. The cytokine

RANKL produced by positively selected thymocytes fosters medullary thymic epithelial cells that express autoimmune regulator. *Immunity* 29:438-450.

Hinterberger, M., M. Aichinger, O. Prazeres da Costa, D. Voehringer, R. Hoffmann, and L. Klein. 2010. Autonomous role of medullary thymic epithelial cells in central CD4(+) T cell tolerance. *Nat Immunol* 11:512-519.

Hubert, F.X., S.A. Kinkel, G.M. Davey, B. Phipson, S.N. Mueller, A. Liston, A.I. Proietto, P.Z. Cannon, S. Forehan, G.K. Smyth, L. Wu, C.C. Goodnow, F.R. Carbone, H.S. Scott, and W.R. Heath. 2011. Aire regulates the transfer of antigen from mTECs to dendritic cells for induction of thymic tolerance. *Blood* 118:2462-2472.

Hubert, F.X., S.A. Kinkel, K.E. Webster, P. Cannon, P.E. Crewther, A.I. Proeitto, L. Wu, W.R. Heath, and H.S. Scott. 2008. A specific anti-Aire antibody reveals aire expression is restricted to medullary thymic epithelial cells and not expressed in periphery. *J Immunol* 180:3824-3832.

Husebye, E.S., M.S. Anderson, and O. Kämpe. 2018. Autoimmune Polyendocrine Syndromes. *N Engl J Med* 378:2543-2544.

Jones, R., E.J. Cosway, C. Willis, A.J. White, W.E. Jenkinson, H.J. Fehling, G. Anderson, and D.R. Withers. 2018. Dynamic changes in intrathymic ILC populations during murine neonatal development. *Eur J Immunol* 48:1481-1491.

Kawabe, T., T. Naka, K. Yoshida, T. Tanaka, H. Fujiwara, S. Suematsu, N. Yoshida, T. Kishimoto, and H. Kikutani. 1994. The immune responses in CD40-deficient mice: impaired immunoglobulin class switching and germinal center formation. *Immunity* 1:167-178.

Kirberg, J., A. Baron, S. Jakob, A. Rolink, K. Karjalainen, and H. von Boehmer. 1994. Thymic selection of CD8+ single positive cells with a class II major histocompatibility complex-restricted receptor. *J Exp Med* 180:25-34.

Klein, L., B. Kyewski, P.M. Allen, and K.A. Hogquist. 2014. Positive and negative selection of the T cell repertoire: what thymocytes see (and don't see). *Nat Rev Immunol* 14:377-391.

Klose, C.S., E.A. Kiss, V. Schwierzeck, K. Ebert, T. Hoyler, Y. d'Hargues, N. Goppert, A.L. Croxford, A. Waisman, Y. Tanriver, and A. Diefenbach. 2013. A T-bet gradient controls the fate and function of CCR6-RORgammat+ innate lymphoid cells. *Nature* 494:261-265.

Kuroda, N., T. Mitani, N. Takeda, N. Ishimaru, R. Arakaki, Y. Hayashi, Y. Bando, K. Izumi, T. Takahashi, T. Nomura, S. Sakaguchi, T. Ueno, Y. Takahama, D. Uchida, S. Sun, F. Kajiura, Y. Mouri, H. Han, A. Matsushima, G. Yamada, and M. Matsumoto. 2005. Development of autoimmunity against transcriptionally unrepressed target antigen in the thymus of Aire-deficient mice. *Journal of immunology* 174:1862-1870.

Kyewski, B., and L. Klein. 2006. A central role for central tolerance. *Annu Rev Immunol* 24:571-606.

Laan, M., K. Kisand, V. Kont, K. Moll, L. Tserel, H.S. Scott, and P. Peterson. 2009. Autoimmune regulator deficiency results in decreased expression of CCR4 and CCR7 ligands and in delayed migration of CD4+ thymocytes. *J Immunol* 183:7682-7691.

LaFlam, T.N., G. Seumois, C.N. Miller, W. Lwin, K.J. Fasano, M. Waterfield, I. Proekt, P. Vijayanand, and M.S. Anderson. 2015. Identification of a novel cis-regulatory element essential for immune tolerance. *J Exp Med* 212:1993-2002.

Lei, Y., A.M. Ripen, N. Ishimaru, I. Ohigashi, T. Nagasawa, L.T. Jeker, M.R. Bosl, G.A. Hollander, Y. Hayashi, W. Malefyt Rde, T. Nitta, and Y. Takahama. 2011. Aire-dependent production of XCL1 mediates medullary accumulation of thymic dendritic cells and contributes to regulatory T cell development. *J Exp Med* 208:383-394.

Li, J., I. Sarosi, X.Q. Yan, S. Morony, C. Capparelli, H.L. Tan, S. McCabe, R. Elliott, S. Scully, G. Van, S. Kaufman, S.C. Juan, Y. Sun, J. Tarpley, L. Martin, K. Christensen, J. McCabe, P. Kostenuik, H. Hsu, F. Fletcher, C.R. Dunstan, D.L. Lacey, and W.J. Boyle. 2000. RANK is the intrinsic hematopoietic cell surface receptor that controls osteoclastogenesis and regulation of bone mass and calcium metabolism. *Proc Natl Acad Sci U S A* 97:1566-1571.

Lindh, E., S.M. Lind, E. Lindmark, S. Hassler, J. Perheentupa, L. Peltonen, O. Winqvist, and M.C. Karlsson. 2008. AIRE regulates T-cell-independent B-cell responses through BAFF. *Proc Natl Acad Sci U S A* 105:18466-18471.

Lochner, M., L. Peduto, M. Cherrier, S. Sawa, F. Langa, R. Varona, D. Riethmacher, M. Si-Tahar, J.P. Di Santo, and G. Eberl. 2008. In vivo equilibrium of proinflammatory IL-17+ and regulatory IL-10+ Foxp3+ RORgamma t+ T cells. *J Exp Med* 205:1381-1393.

Luci, C., A. Reynders, Ivanov, II, C. Cognet, L. Chiche, L. Chasson, J. Hardwigsen, E. Anguiano, J. Banchereau, D. Chaussabel, M. Dalod, D.R. Littman, E. Vivier, and E. Tomasello. 2009. Influence of the transcription factor RORgammat on the development of NKp46+ cell populations in gut and skin. *Nat Immunol* 10:75-82.

Mackley, E.C., S. Houston, C.L. Marriott, E.E. Halford, B. Lucas, V. Cerovic, K.J. Filbey, R.M. Maizels, M.R. Hepworth, G.F. Sonnenberg, S. Milling, and D.R. Withers. 2015. CCR7-dependent trafficking of RORgamma(+) ILCs creates a unique microenvironment within mucosal draining lymph nodes. *Nat Commun* 6:5862.

Mathis, D., and C. Benoist. 2007. A decade of AIRE. *Nat Rev Immunol* 7:645-650.

Meredith, M., D. Zemmour, D. Mathis, and C. Benoist. 2015. Aire controls gene expression in the thymic epithelium with ordered stochasticity. *Nat Immunol* 16:942-949.

Montaldo, E., K. Juelke, and C. Romagnani. 2015. Group 3 innate lymphoid cells (ILC3s): Origin, differentiation, and plasticity in humans and mice. *Eur J Immunol* 45:2171-2182.

Nedjic, J., M. Aichinger, N. Mizushima, and L. Klein. 2009. Macroautophagy, endogenous MHC II loading and T cell selection: the benefits of breaking the rules. *Curr Opin Immunol* 21:92-97.

Nishikawa, Y., F. Hirota, M. Yano, H. Kitajima, J. Miyazaki, H. Kawamoto, Y. Mouri, and M. Matsumoto. 2010. Biphasic Aire expression in early embryos and in medullary thymic epithelial cells before end-stage terminal differentiation. *J Exp Med* 207:963-971.

Nutt, S.L., B. Heavey, A.G. Rolink, and M. Busslinger. 1999. Commitment to the B-lymphoid lineage depends on the transcription factor Pax5. *Nature* 401:556-562.

Peterson, P., T. Org, and A. Rebane. 2008. Transcriptional regulation by AIRE: molecular mechanisms of central tolerance. *Nat Rev Immunol* 8:948-957.

Pfaffl, M.W. 2001. A new mathematical model for relative quantification in real-time RT-PCR. *Nucleic Acids Res* 29:e45.

Poliani, P.L., K. Kisand, V. Marrella, M. Ravanini, L.D. Notarangelo, A. Villa, P. Peterson, and F. Facchetti. 2010. Human peripheral lymphoid tissues contain autoimmune regulator-expressing dendritic cells. *Am J Pathol* 176:1104-1112.

Ramsey, C., O. Winqvist, L. Puhakka, M. Halonen, A. Moro, O. Kampe, P. Eskelin, M. Pelto-Huikko, and L. Peltonen. 2002. Aire deficient mice develop multiple features of APECED phenotype and show altered immune response. *Hum Mol Genet* 11:397-409.

Roberts, N.A., A.J. White, W.E. Jenkinson, G. Turchinovich, K. Nakamura, D.R. Withers, F.M. McConnell, G.E. Desanti, C. Benezech, S.M. Parnell, A.F. Cunningham, M. Paolino, J.M. Penninger, A.K. Simon, T. Nitta, I. Ohigashi, Y.

Takahama, J.H. Caamano, A.C. Hayday, P.J. Lane, E.J. Jenkinson, and G. Anderson. 2012. Rank signaling links the development of invariant gammadelta T cell progenitors and Aire(+) medullary epithelium. *Immunity* 36:427-437.

Robinette, M.L., A. Fuchs, V.S. Cortez, J.S. Lee, Y. Wang, S.K. Durum, S. Gilfillan, M. Colonna, and C. Immunological Genome. 2015. Transcriptional programs define molecular characteristics of innate lymphoid cell classes and subsets. *Nat Immunol* 16:306-317.

Rossi, S.W., M.Y. Kim, A. Leibbrandt, S.M. Parnell, W.E. Jenkinson, S.H. Glanville, F.M. McConnell, H.S. Scott, J.M. Penninger, E.J. Jenkinson, P.J. Lane, and G. Anderson. 2007. RANK signals from CD4(+)3(-) inducer cells regulate development of Aire-expressing epithelial cells in the thymic medulla. *J Exp Med* 204:1267-1272.

Sansom, S.N., N. Shikama-Dorn, S. Zhanybekova, G. Nusspaumer, I.C. Macaulay, M.E. Deadman, A. Heger, C.P. Ponting, and G.A. Hollander. 2014. Population and single-cell genomics reveal the Aire dependency, relief from Polycomb silencing, and distribution of self-antigen expression in thymic epithelia. *Genome Res* 24:1918-1931.

Satoh-Takayama, N., L. Dumoutier, S. Lesjean-Pottier, V.S. Ribeiro, O. Mandelboim, J.C. Renauld, C.A. Vosshenrich, and J.P. Di Santo. 2009. The natural cytotoxicity receptor NKp46 is dispensable for IL-22-mediated innate intestinal immune defense against Citrobacter rodentium. *J Immunol* 183:6579-6587.

Schaller, C.E., C.L. Wang, G. Beck-Engeser, L. Goss, H.S. Scott, M.S. Anderson, and M. Wabl. 2008. Expression of Aire and the early wave of apoptosis in spermatogenesis. *J Immunol* 180:1338-1343.

Seehus, C.R., P. Aliahmad, B. de la Torre, I.D. Iliev, L. Spurka, V.A. Funari, and J. Kaye. 2015. The development of innate lymphoid cells requires TOX-dependent generation of a common innate lymphoid cell progenitor. *Nat Immunol* 16:599-608.

Spits, H., D. Artis, M. Colonna, A. Diefenbach, J.P. Di Santo, G. Eberl, S. Koyasu, R.M. Locksley, A.N. McKenzie, R.E. Mebius, F. Powrie, and E. Vivier. 2013. Innate lymphoid cells--a proposal for uniform nomenclature. *Nat Rev Immunol* 13:145-149.

Stoppelenburg, A.J., J.H. von Hegedus, R. Huis in't Veld, L. Bont, and M. Boes. 2014. Defective control of vitamin D receptor-mediated epithelial STAT1 signalling predisposes to severe respiratory syncytial virus bronchiolitis. *J Pathol* 232:57-64.

Su, M.A., K. Giang, K. Zumer, H. Jiang, I. Oven, J.L. Rinn, J.J. Devoss, K.P. Johannes, W. Lu, J. Gardner, A. Chang, P. Bubulya, H.Y. Chang, B.M. Peterlin, and M.S. Anderson. 2008. Mechanisms of an autoimmunity syndrome in mice caused by a dominant mutation in Aire. *J Clin Invest* 118:1712-1726.

von Burg, N., S. Chappaz, A. Baerenwaldt, E. Horvath, S. Bose Dasgupta, D. Ashok, J. Pieters, F. Tacchini-Cottier, A. Rolink, H. Acha-Orbea, and D. Finke. 2014. Activated group 3 innate lymphoid cells promote T-cell-mediated immune responses. *Proc Natl Acad Sci U S A* 111:12835-12840.

Wang, X., M. Laan, R. Bichele, K. Kisand, H.S. Scott, and P. Peterson. 2012. Post-Aire maturation of thymic medullary epithelial cells involves selective expression of keratinocyte-specific autoantigens. *Front Immunol* 3:19.

Yamano, T., J. Nedjic, M. Hinterberger, M. Steinert, S. Koser, S. Pinto, N. Gerdes, E. Lutgens, N. Ishimaru, M. Busslinger, B. Brors, B. Kyewski, and L. Klein. 2015. Thymic B Cells Are Licensed to Present Self Antigens for Central T Cell Tolerance Induction. *Immunity* 42:1048-1061.

Yano, M., N. Kuroda, H. Han, M. Meguro-Horike, Y. Nishikawa, H. Kiyonari, K. Maemura, Y. Yanagawa, K. Obata, S. Takahashi, T. Ikawa, R. Satoh, H. Kawamoto, Y. Mouri, and M. Matsumoto. 2008. Aire controls the differentiation program of thymic epithelial cells in the medulla for the establishment of self-tolerance. *J Exp Med* 205:2827-2838.

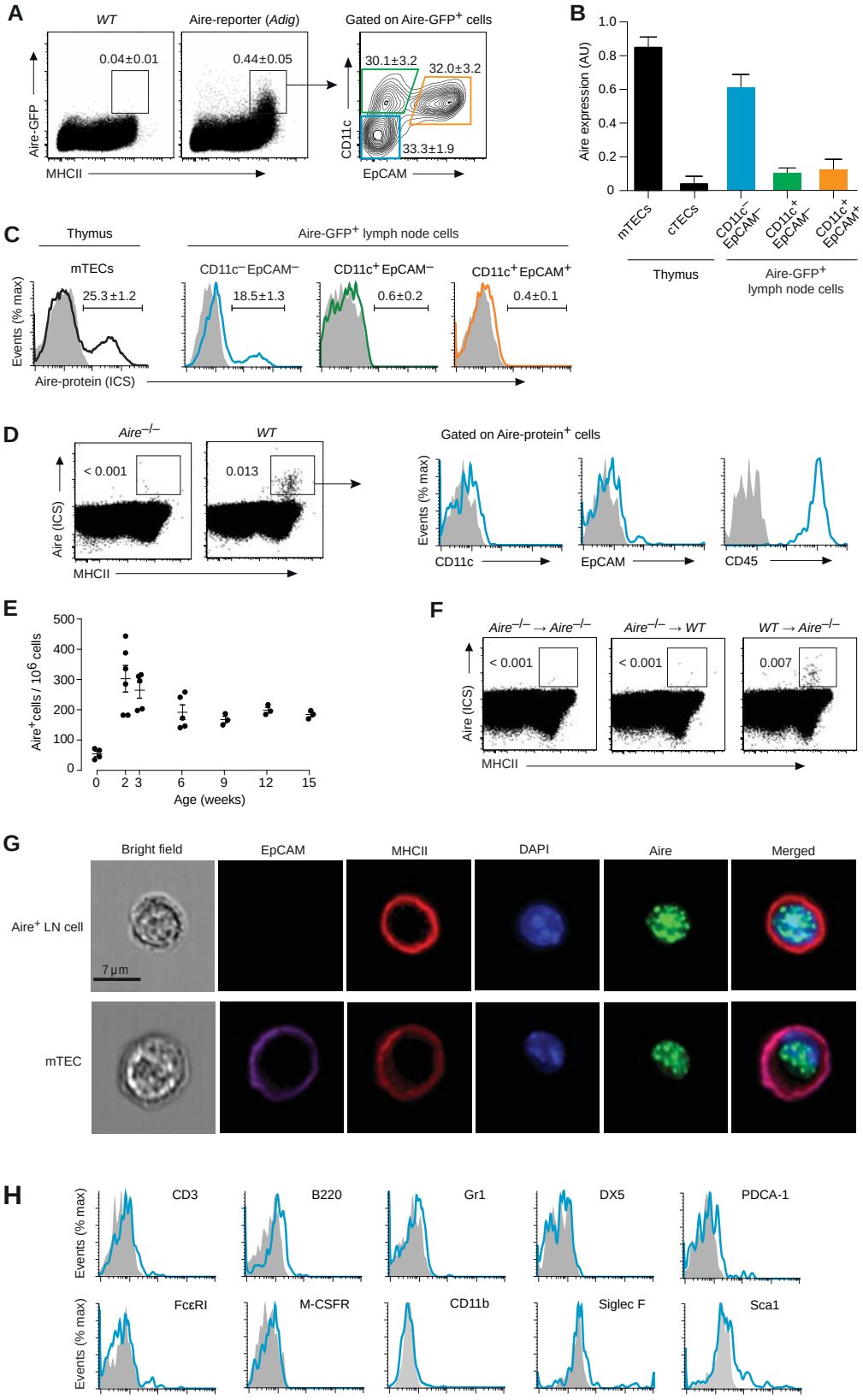

Figure 1 | Yamano, Dobes et al.

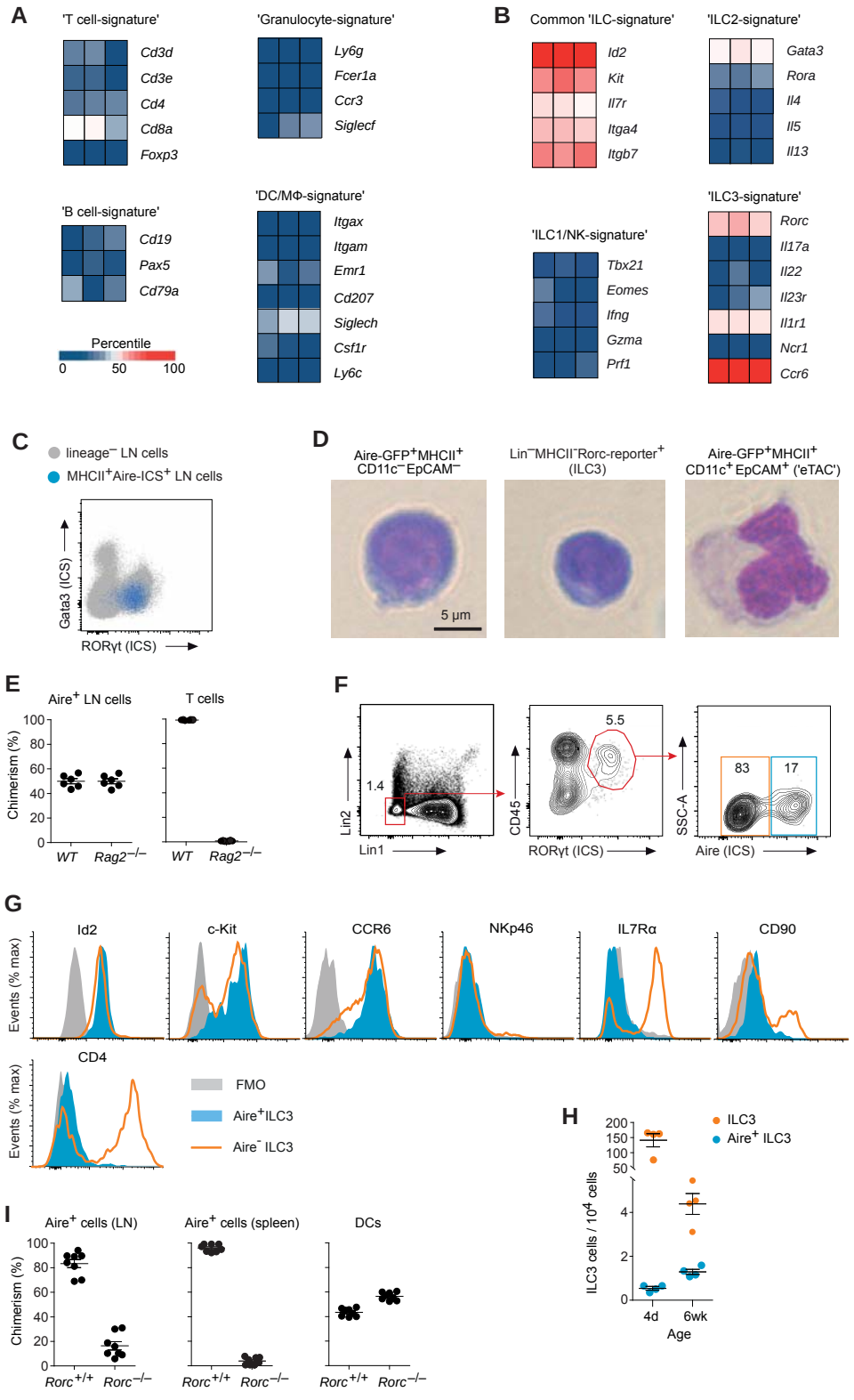

Figure 2 | Yamano, Dobes et al.

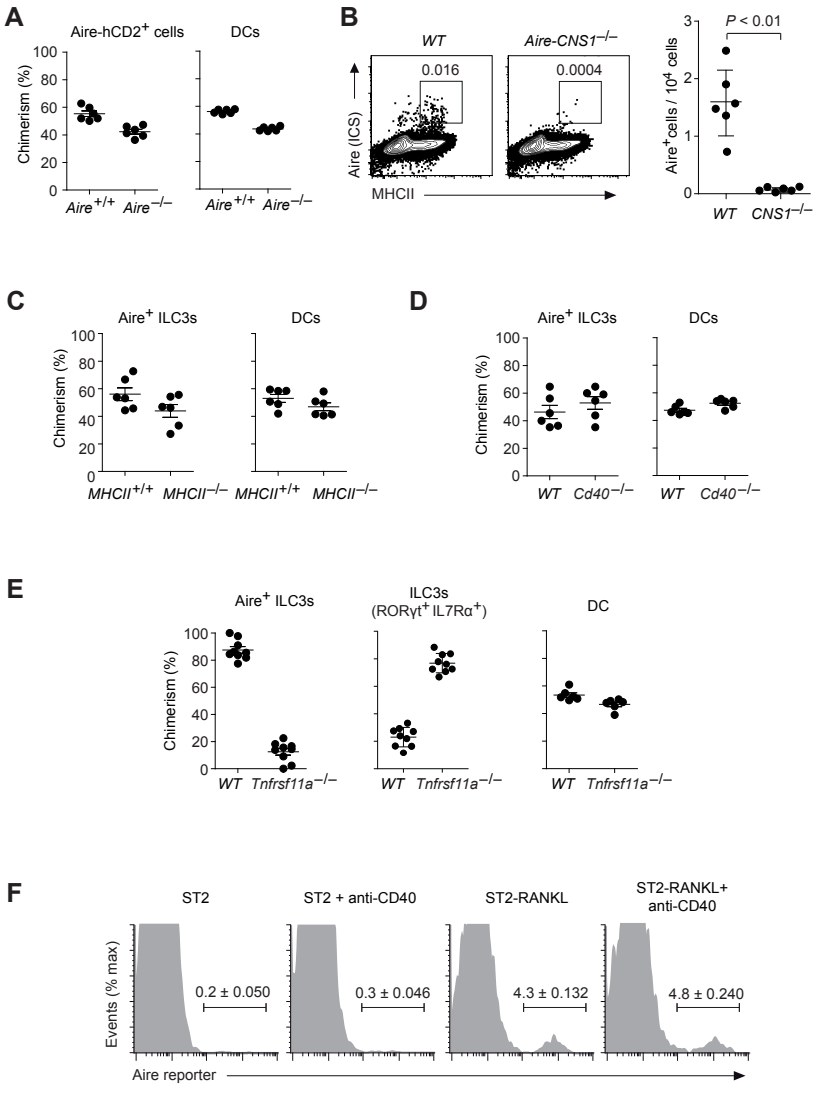

Figure 3 | Yamano, Dobes et al.

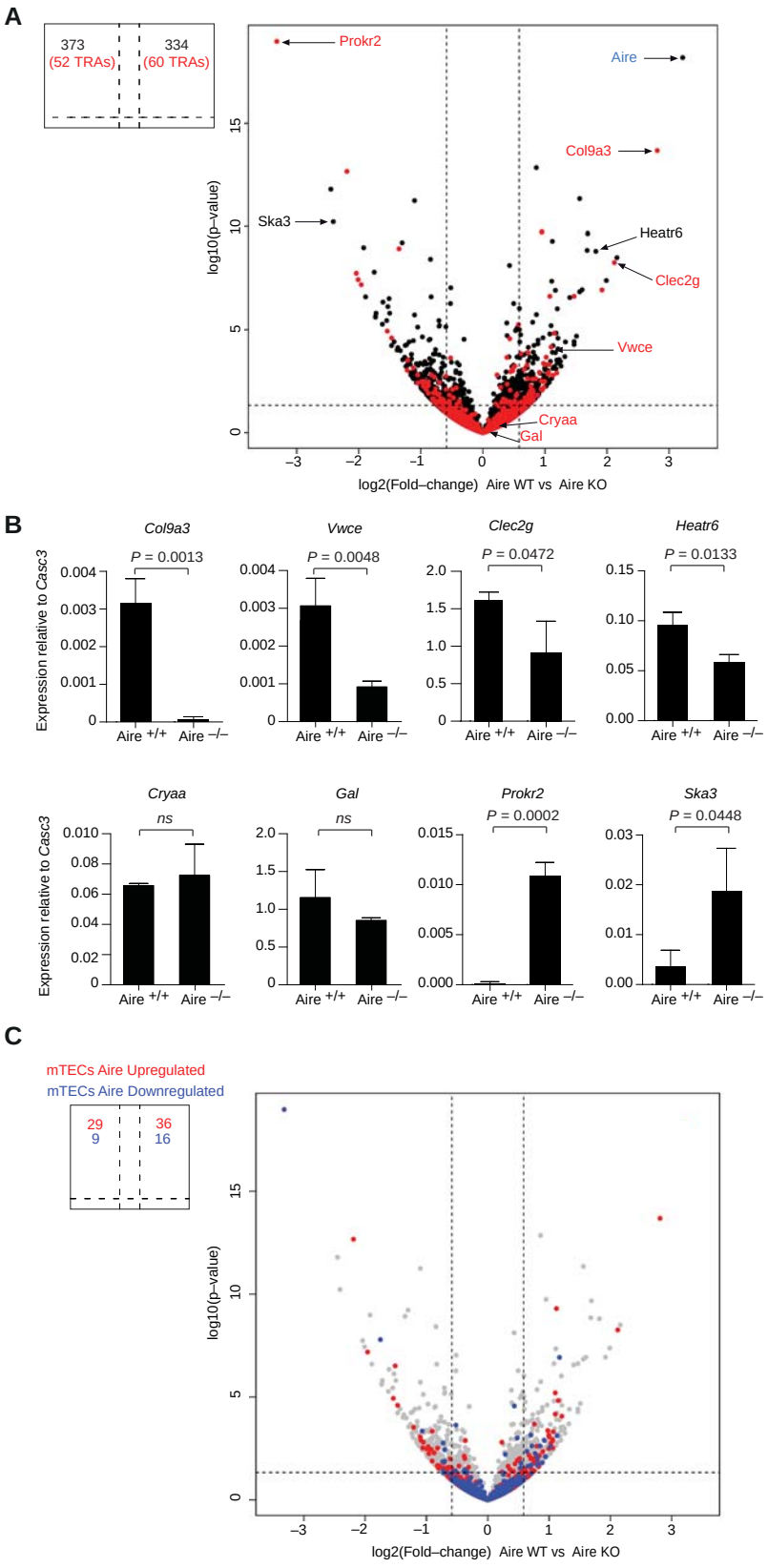

Figure 4 | Yamano, Dobes et al.

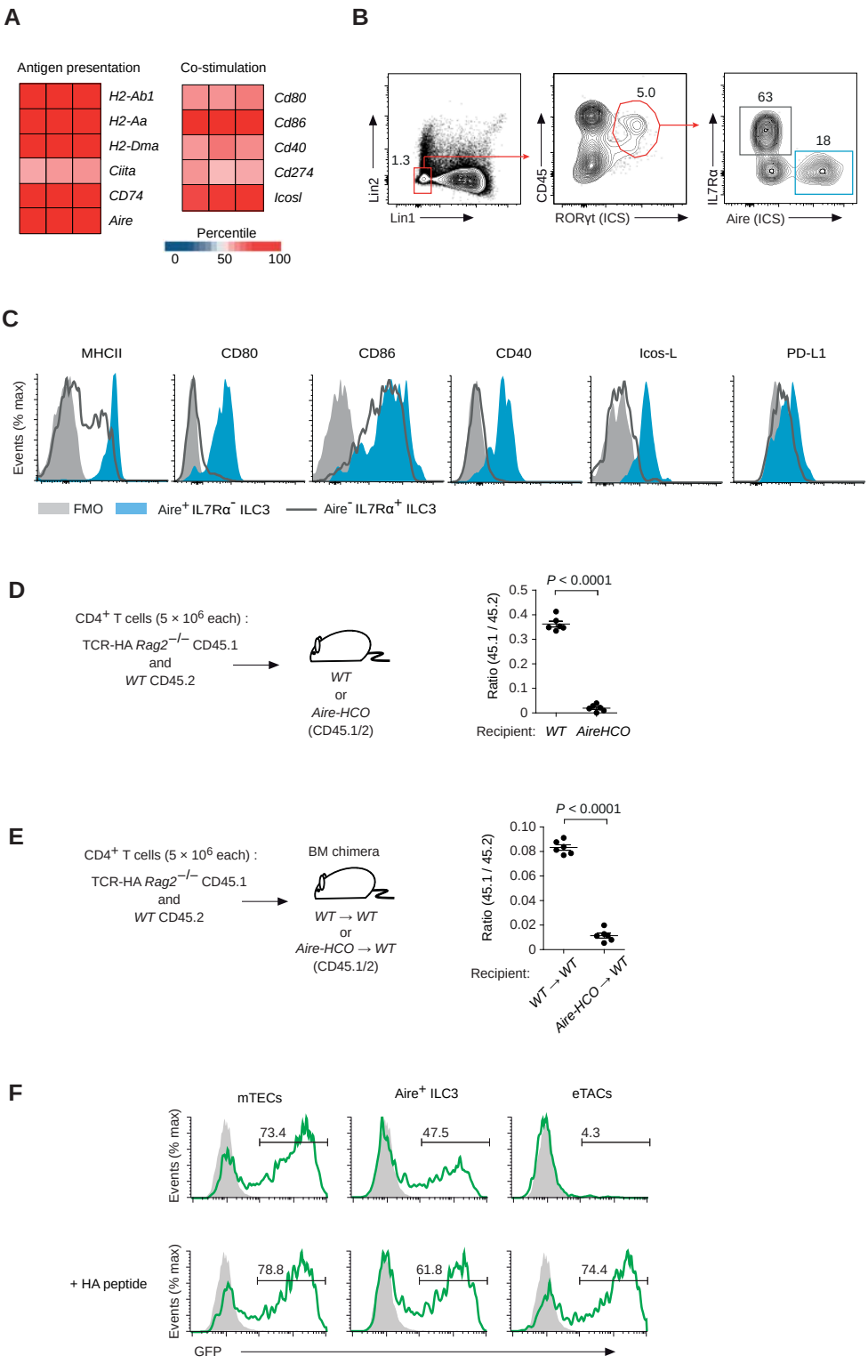

Figure 5 | Yamano, Dobes et al.

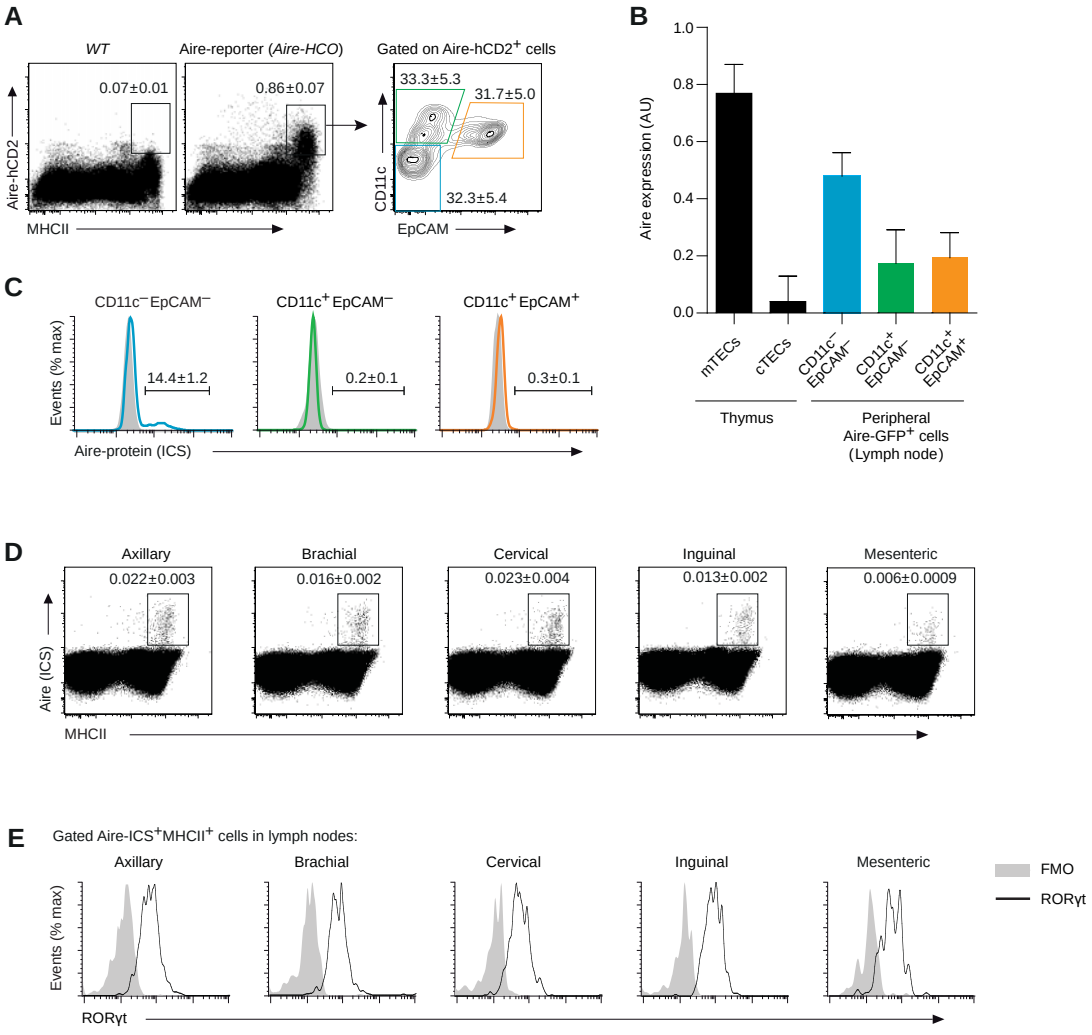

Figure S1, related to Figure 1 | Phenotype of Aire expressing cells in lymph nodes. (A) Expression of human CD2 (hCD2) reporter and MHCII in total lymph node cells (isolated from peripheral lymph nodes) from Aire-HCO Aire-reporter mice and WT controls. The dot plot on the right shows staining for CD11c and EpCAM on gated Aire-hCD2^{+}MHCII^{+} cells. The average frequency of cells in the respective gates is indicated (representative of n ≥ 3 each). (B) Aire mRNA in subsets of Aire-hCD2^{+} lymph node cells from Adig mice sorted according to the expression of CD11c and EpCAM as in (A), in comparison to mTECs and cTECs. Data shown is of mean values ± SEM of triplicates (AU; arbitrary units). (C) Intracellular staining (ICS) for Aire protein in subsets of Aire-hCD2^{+} lymph node cells from Aire-HCO mice. Cells were gated according to the expression of CD11c and EpCAM as in (A). The average frequency of Aire-ICS^{+} cells is indicated (n = 3). (D) ICS for Aire protein and surface expression of MHCII in total lymph node cells isolated from differentially localized lymph nodes (n = 3). (E) Histograms of the Rorγt ICS of MHCII^{+}Aire-ICS^{+} cells gated according to (D) (n = 3).

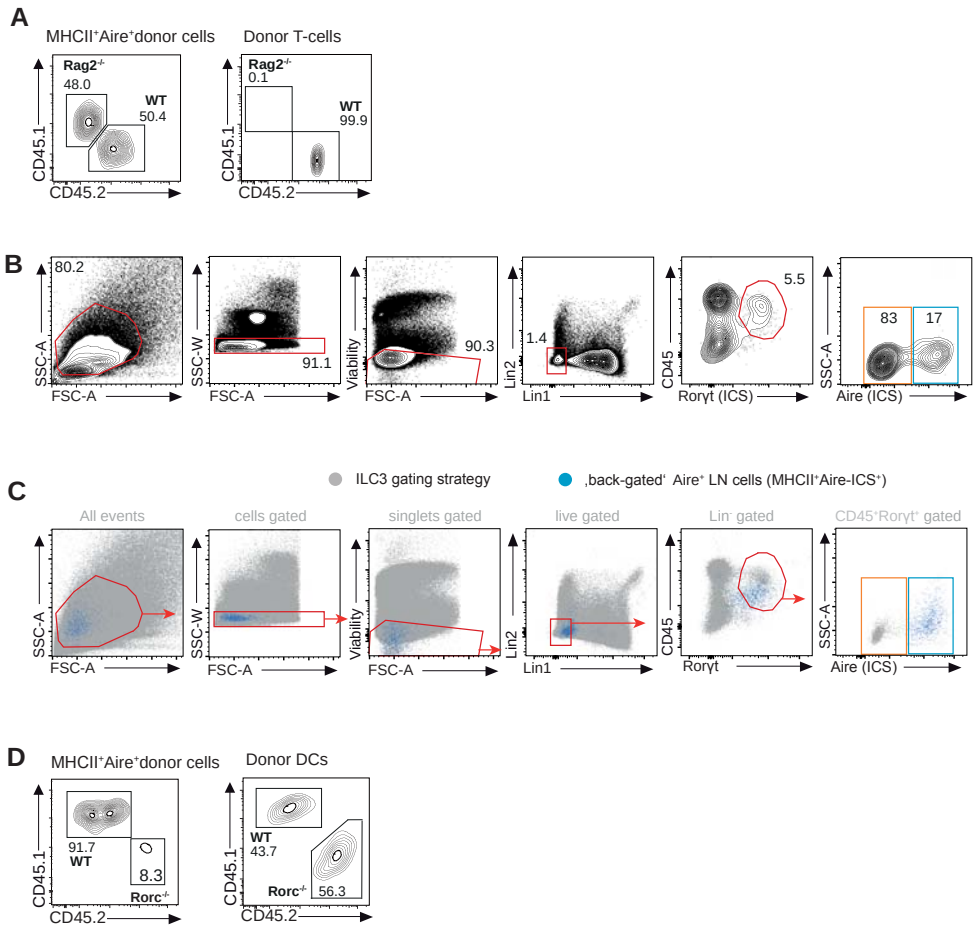

Figure S2, related to Figure 2 | Representative gating strategies of Aire^{+}ILC3 cells. (A) Representative gating strategy, related to Figure 2E, of MHCII^{+}Aire-ICS^{+} donor cells (left dot plot) and donor T-cells (right dot plot) isolated from peripheral lymph node (pLN) of mixed bonne marrow chimeras (WT:Rag2$^{-/-}$). Donor cells were gated as CD45.1 (Rag2$^{-/-}$) and CD45.2 (WT) single positive. (B) Complete gating strategy of pLN ILC3 cells related to figure 2F. Cell suspension was sequentially gated according to FSC-A and SSC-A, singlets and live cells. Live cells were then gated as lineage negative (Lin1 = CD3, CD19, B220, Gr-1, Lin2 = CD11c and CD11b) from which ILC3 cells were gated as double positive for CD45 and intracellular (ICS) Roryt. Aire^{+}ILC3 were distinguished from the 'canonical' ILC3 by ICS Aire staining. (C) Back-gating of Aire^{+} LN cells to ILC3 gating strategy shown in B (Gray cells). Specifically, Aire^{+} LN cells (Blue cells) were independently gated as Aire-ICS^{+}MHCII^{+} (shown in Figure 1D). (D) Representative gating strategy, related to Figure 2I, of MHCII^{+}Aire-ICS^{+} donor cells (left dot plot) and donor dendritic cell (DCs) (right dot plot) isolated from the spleen of mixed bonne marrow chimeras (WT:Rorc$^{-/-}$). Donor cells were gated as CD45.1 (WT) and CD45.2 (Rorc$^{-/-}$) single positive.

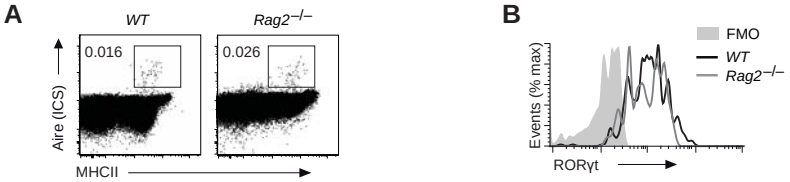

Supplementary Figure S3 | Rag2 is dispensable for Aire^{+} ILC3 development. (A) Intracellular staining (ICS) for Aire protein and surface expression of MHCII in total lymph node cells from WT controls and Rag2$^{-/-}$ mice (representative of n ≥ 3 each). **(B)** Histograms comparing Rorγt ICS in cells gated as in (A) isolated from WT controls and Rag2$^{-/-}$ mice (representative of n ≥ 3 each).

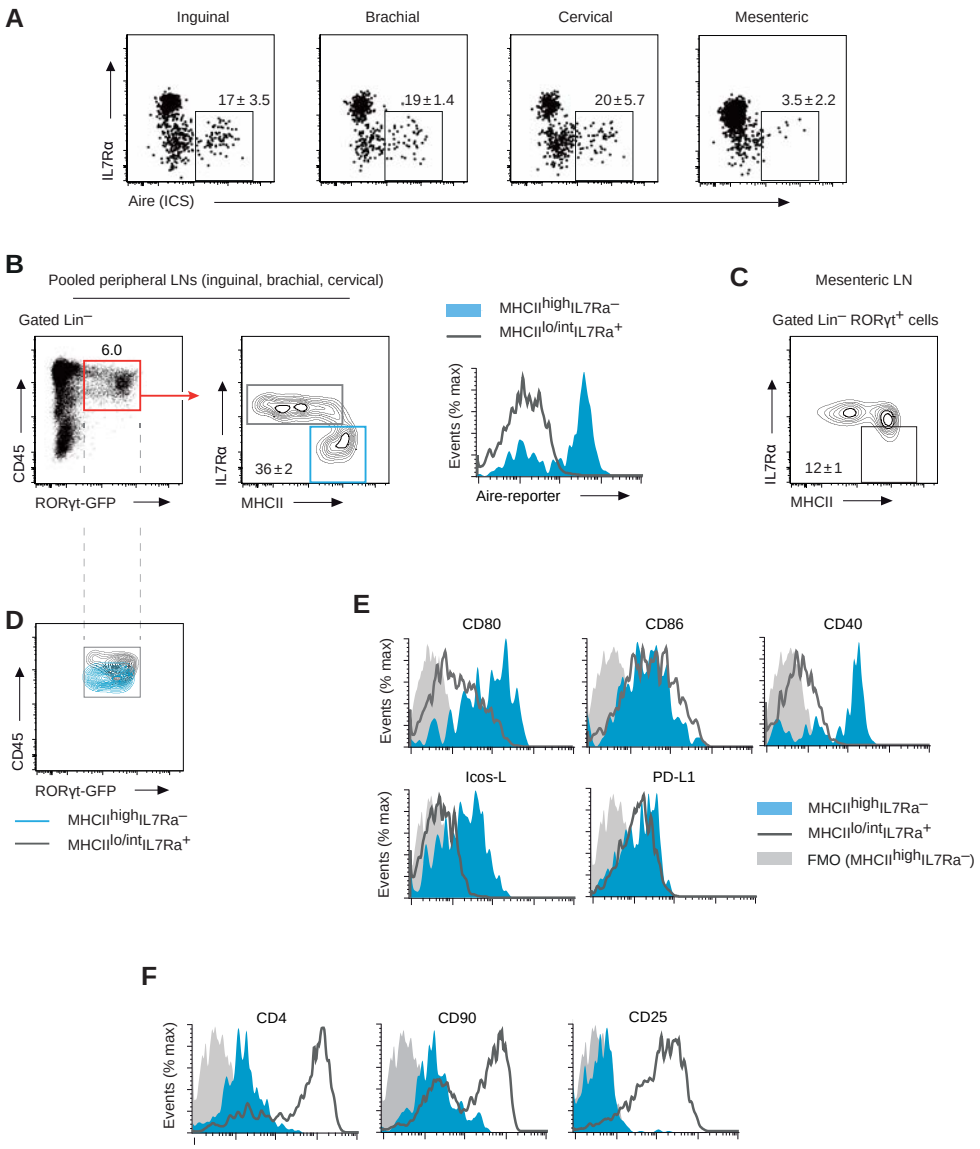

Figure S4, related to Figure 5 | MHCII^{high}IL7Ra^{-} ILC3s express Aire and co-stimulatory molecules. (A) Expression of IL7Ra and Aire (ICS) in gated Lin^{-} (CD3, CD8, CD19, CD11b, CD11c, Ter119, Gr-1, FcεR) RORγt(ICS)$^{+}$ cells from different peripheral and mesenteric lymph nodes of WT mice. (B) Expression of IL7Ra and MHC class II in gated Lin^{-}CD45^{+}RORγt-GFP^{+} cells from pooled peripheral lymph nodes of RORγt-GFP/Aire-hCD2 double-reporter mice. The histogram overlay on the right shows Aire reporter expression in gated MHCII$^{lo/int}$IL7Ra^{+} (open grey) and MHCII^{high}IL7Ra^{-} cells (filled blue). (C) Expression of IL7Ra and MHC class II in gated Lin^{-}CD45^{+}RORγt^{+} cells from mesenteric lymph nodes. (D) Overlay of CD45 and RORγt-reporter expression in MHCII$^{lo/int}$IL7Ra^{+} (grey) and MHCII^{high}IL7Ra^{-} ILC3s (blue) from pooled peripheral LNs back-gated from (B). (E) Expression of co-stimulatory or co-inhibitory molecules by gated MHCII$^{lo/int}$IL7Ra^{+} (open grey) and MHCII^{high}IL7Ra^{-} ILC3s (filled blue) from pooled peripheral LNs, gated as in (B). (F) Expression of CD4, CD90 and CD25 by gated MHCII$^{lo/int}$IL7Ra^{+} (open grey) and MHCII^{high}IL7Ra^{-} ILC3s (filled blue) from pooled peripheral LNs gated as in (B).